The Paleoproterozoic fossil record: Implications for the evolution of the biosphere during Earth's middle-age

Emmanuelle J. Javaux, Kevin Lepot

Earth-Science Reviews 176 (2018) 68–86

Contents lists available at ScienceDirect

Earth-Science Reviews

journal homepage: www.elsevier.com/locate/earscirev

Invited review

The Paleoproterozoic fossil record: Implications for the evolution of the biosphere during Earth's middle-age

Emmanuelle J. Javaux[a,*], Kevin Lepot[b]

[a] University of Liège, Department of Geology, Palaeobiogeology-Palaeobotany-Palaeopalynology, 14, allée du 6 Août B18, quartier AGORA, 4000 Liège, (Sart-Tilman), Belgium

[b] Université de Lille, CNRS, Université Littoral Côte d'Opale, Laboratoire d'Océanologie et de Géosciences UMR8187, Cité Scientifique, SN5, 59655 Villeneuve d'Ascq, France

ARTICLE INFO

Keywords:
Paleoproterozoic
Microfossils
Iron formations
Prokaryotes
Eukaryotes
Cyanobacteria

ABSTRACT

The Paleoproterozoic (2.5–1.6 Ga) Era is a decisive time in Earth and life history. The paleobiological record (microfossils, stromatolites, biomarkers and isotopes) illustrates the biosphere evolution during a time of transitional oceanic and atmosphere chemistries. Benthic microfossil assemblages are recorded in a variety of oxygenated, sulfidic, and ferruginous environments representative of the spatial heterogeneities and temporal variations characteristic of this Era. The microfossil assemblages include iron-metabolizing and/or iron-tolerant prokaryotes, sulfur-metabolizing prokaryotes, cyanobacteria, other undetermined prokaryotes, and eukaryotes. The undetermined microfossils represent a majority of the assemblages and thus raise a challenge to determine the nature and role of microorganisms in these changing environments. Despite the early evolution of the eukaryotic cellular toolkit, early eukaryotic crown group diversification may have been restrained in the Paleoproterozoic by ocean chemistry conditions, but it increased during the late Mesoproterozoic–early Neoproterozoic despite the continuation of similar conditions through the (miscalled) "boring billion", then amplified significantly (but perhaps within lower taxonomic levels), with the demise of euxinic conditions and increase in ecological complexity.

The emerging picture is one of a changing and more complex biosphere in which the three domains of life, Archaea, Bacteria and Eukarya, were diversifying in various ecological niches marked by the diversification of identified microfossils, stromatolites, increasing abundance of preserved biomarkers, and appearance of macroscopic problematic fossils or trace fossils.

1. Introduction

The Paleoproterozoic (2.5–1.6 Ga: billion years) Era is a decisive time in Earth and life history. Drastic environmental changes affected ocean and atmosphere chemistry, including step-wise and possibly fluctuating oxygenation (Lyons et al., 2014), the Huronian glaciations (three ice ages, between 2.45 and 2.22 Ga; Barley et al., 2005), large organic carbon deposits during the Lomagundi-Jatuli event (Melezhik et al., 2013) at ~2.3–2.06 Ga, an alternation of enhanced magmatic activity (maxima at ~2.7 Ga and ~1.9 Ga) and more quiescent periods (2.45–2.2 Ga) (Condie et al., 2009) (Fig. 1). These environmental changes may have had profound consequences on life's diversification by modifying the physico-chemical conditions and diversity of ecological niches. For example, decrease in submarine volcanism may have limited the flux of Fe^{2+}, H_2 and H_2S, hence limiting major sinks acting against O_2 accumulation between 2.45 and 2.22 Ga (Kump and Barley, 2007).

Life also deeply marked Earth's planetary evolution during this Era (Fig. 1). The Archean–Proterozoic transition started with the so-called great oxidation event (GOE) between 2.48 and 2.32 Ga (Bekker et al., 2004; Hannah et al., 2004), when molecular oxygen accumulated sufficiently in the ocean and atmosphere to be detected widely by a variety of geological and geochemical proxies (Bekker et al., 2004; Sessions et al., 2009). These proxies provide a minimum age for the advent of oxygenic photosynthesis by cyanobacteria on the planetary scale but earlier local oxygenated oases may have occurred in photic zones where oxygenic cyanobacteria first developed. Possible origin of oxygenic photosynthesis (by cyanobacteria) has been suggested as early as 3.7 Ga based on carbon and Pb isotopic memory of past U/Th ratios (Rosing and Frei, 2004), but see Buick (2008); 3.2 Ga based on thick and widespread deposits of kerogenous black shales (Buick, 2008); 2.9 Ga based on S-isotopes (Ono et al., 2006). More direct tracers linked with geochemical reactions requiring dioxygen can be tracked back as far as

* Corresponding author.
E-mail addresses: Ej.javaux@ulg.ac.be (E.J. Javaux), Kevin.Lepot@univ-lille1.fr (K. Lepot).

http://dx.doi.org/10.1016/j.earscirev.2017.10.001
Received 21 September 2017; Received in revised form 3 October 2017; Accepted 3 October 2017
Available online 04 October 2017

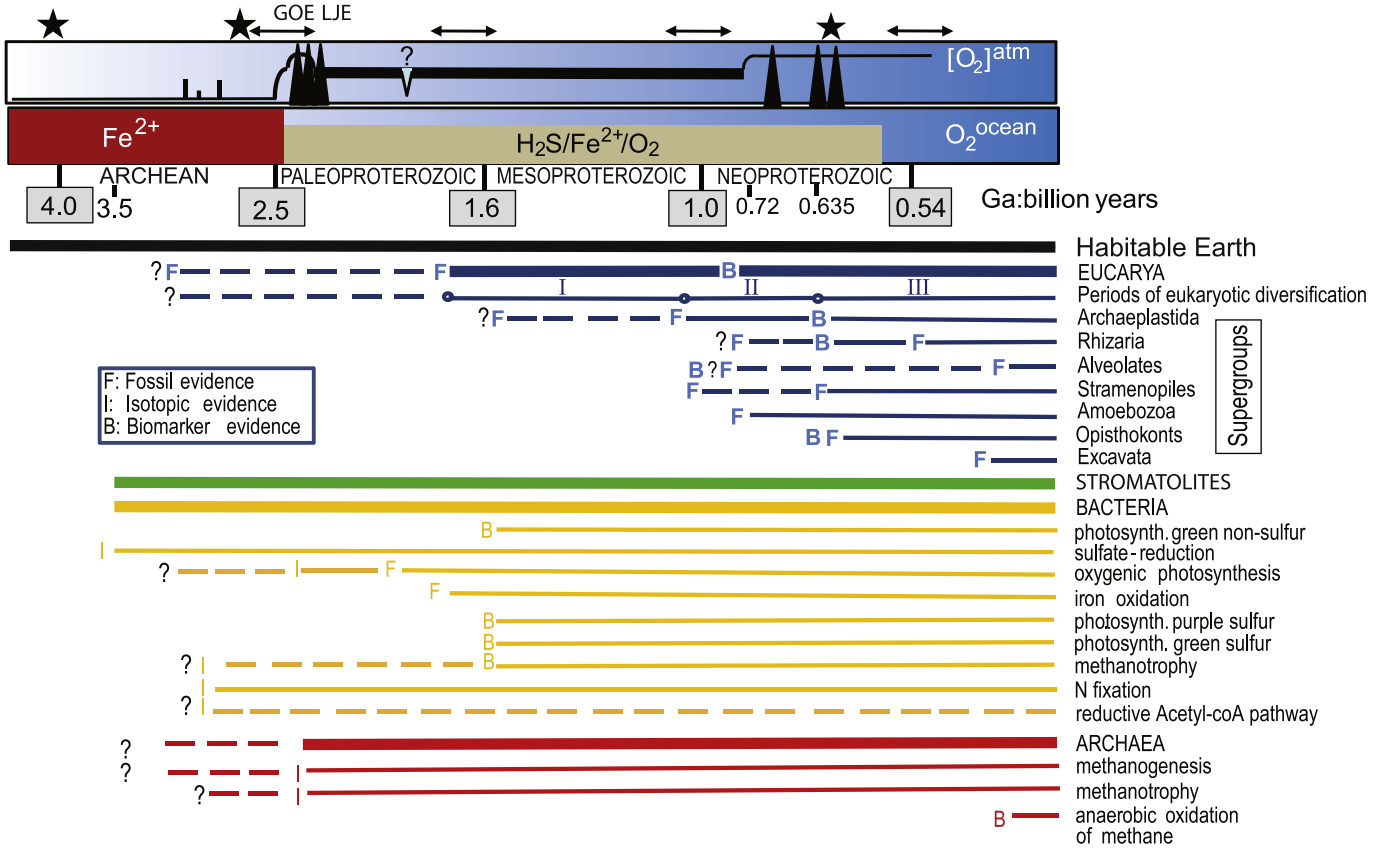

Fig. 1. Summary of changing physico-chemical conditions in the Archean and Proterozoic ocean and atmosphere, and fossil, biomarker and isotopic evidence for the record of Eukaryotic supergroups, and Bacteria and Archaea metabolisms (black stars: large meteoritic impacts; double-headed arrows: supercontinent formation and break-up; black triangles: widespread glaciations; GOE: great oxidation event; LJE: Lomagundi-Jatuli event). References cited in the text and in Javaux (2011).

3.0–2.8 Ga ago based on chromium isotopes (Crowe et al., 2013; Frei et al., 2009); 2.95 Ga based on Mo isotopes (Planavsky et al., 2014); and 2.5 Ga based on molybdenum and rhenium data (Anbar et al., 2007). However, some molecular phylogenies suggest that oxygenic photosynthesis appeared close to the GOE (Shih et al., 2017) and alternative hypotheses for earlier "whiffs" in dioxygen have been suggested as other biotic or abiotic processes are possible (Fischer et al., 2016). Recently, the biomarker evidence for cyanobacteria (and eukaryotes) in Archean rocks (Brocks et al., 2003; Eigenbrode et al., 2008) was reassessed as contamination (French et al., 2015; Rasmussen et al., 2008). Some Paleoproterozoic eukaryote biomarkers have also been discussed as possible contaminants (Brocks et al., 2008; Flannery and George, 2014) and "steranes fading out beyond 800 Ma indicates the absence of a reliable record" (Brocks et al., 2017). Biomarkers for green and purple sulfur bacteria (anoxygenic photosynthesizers) occur in the 1.64 Ga Barney Creek Formation (Brocks et al., 2005). Bacterial sulfate reduction is indicated by S isotopes as early as 3.5 Ga (Shen et al., 2009; Ueno et al., 2008). Limitation of nickel concentration, a key co-factor in several enzymes of methanogens, may have led to decreasing atmospheric methane levels and favored the rise of O_2 in the atmosphere from 2.7 Ga onwards (Konhauser et al., 2009). Enzymatic N-fixation (diazotrophy) is suggested as early as 3.2 Ga (Stüeken et al., 2015). Early cyanobacteria could only fix nitrogen at relatively low O_2 concentrations or rely on other nitrogen fixers (Tomitani et al., 2006). Cyanobacteria likely had to invent a new N_2-fixation machinery that could operate in the presence of the rising O_2, possibly leading to the advent of heterocystous cyanobacterial taxa probably as early as the GOE (Schirrmeister et al., 2013), and possibly supported by Paleoproterozoic microfossils (Tomitani et al., 2006), but see Butterfield (2015b). Active N-cycling was favored by the advent of an aerobic nitrogen cycle possibly as early as 2.7 Ga (Garvin et al., 2009; Thomazo et al., 2011), thereby favoring all heterotrophic microorganisms unable to fix N_2. An increase in primary production and sulfate export to the ocean, both favored by the new oxidative subaerial weathering conditions (Bekker and Holland, 2012), stimulated heterotrophic bacterial sulfate reduction (Canfield, 1998). In combination with N cycling, increase in phosphate extracted during oxidative weathering and active N recycling by heterotrophy stimulated primary photosynthetic production (Bekker and Holland, 2012; Papineau et al., 2013) during the Lomagundi-Jatuli event (~2.3–2.06 Ga). However, increase in primary production led to deposition of organic matter that represented a colossal food source for oxygen-respiring bacteria and heterotrophic sulfate-reducing bacteria, possibly leading to a drop in oxygen and sulfate by ~2.05 Ga (e.g. Canfield et al., 2013; Scott et al., 2014).

The redox state and composition of bottom waters during the Paleoproterozoic may have been periodically and/or locally anoxic, dysoxic or euxinic (Johnston et al., 2009) (Fig. 1). Archean oceans were mostly ferruginous; this condition recurred transiently in bottom to shallow waters around 1.9 Ga, possibly due to a return of intense submarine volcanism (Rasmussen et al., 2012) and associated with the post-Lomagundi decline in oxygen (see review in Lyons et al., 2014). During the so-called "boring billion" (~1.9–1.8 to ~0.8 Ga), these conditions changed into sulfidic (H_2S-rich) anoxic conditions (euxinia) in continental shelf and epicontinental sea settings (Canfield, 1998; Poulton et al., 2010) where intense primary production fed sulfate-reducing bacteria. Euxinia with comparatively low sulfate concentrations may also have occurred in the lower part of the photic zone, at least sporadically, in an oxygen-minimum zone-type setting (OMZ), while the surface waters of the photic zone were moderately oxygenated (10^{-4} to 0.1 PAL: present atmospheric level of oxygen) (Brocks et al., 2005; Lyons et al., 2014; Shen et al., 2002, 2003). However, recent studies suggests that ferruginous conditions in deep waters may have

been more widespread than previously documented during Earth's middle age (1.8–1.0 Ga), and that both euxinic and ferruginous stratified waters may have been common below the oxygenated surface-mixing zone (Planavsky et al., 2011; Poulton et al., 2010). The extent of euxinic conditions may have varied in time and space, occurring in restricted basins, or in oceanic wedges close to continental margins with high productivity. Below the surface layer where oxygenic photosynthesis occurred, euxinic conditions may have been maintained until about 750 Ma, when the return to a ferruginous ocean coeval with the break-up of the supercontinent Rodinia prior to the Sturtian glaciation, is documented by S, C and Fe data (Canfield et al., 2008; Johnston et al., 2010; Sperling et al., 2013). The composition of the bottom and/or OMZ waters may have drastically influenced the nature and distribution of the photosynthetic primary producers. Cyanobacteria may have performed anoxygenic (rather than oxygenic) photosynthesis using H_2S above euxinic layers, or may have been outcompeted by anoxygenic photosynthetic bacteria metabolizing H_2S or Fe^{2+} above ferruginous water (Johnston et al., 2009). Moreover, planktonic cyanobacteria may have suffered from Fe^{2+} toxicity (Swanner et al., 2015) in offshore environments where surface water was directly in contact with ferruginous deeper water, although this Fe^{2+} toxicity may have been alleviated in waters saturated with silica (Mloszewska et al., 2015) or through intracellular Fe-biomineralization (Lepot et al., 2017). In this context, oxygenic photosynthesis may have been dominated by benthic (terrestrial and coastal) cyanobacteria from the late Archean possibly until the end of the “boring billion” (Lalonde and Konhauser, 2015). Nevertheless, cyanobacteria may have known an increase in diversification associated with or preceding the GOE and later during the Paleoproterozoic (Schirrmeister et al., 2013). Similarly, the chemical composition of seawater, including sulfate, iron (Ratti et al., 2011), and trace-metal concentrations (Anbar and Knoll, 2002) during the Paleoproterozoic and “boring-billion” may have regulated the evolution and distribution of eukaryotes and their competition with cyanobacteria in the primary photosynthetic biomass (Knoll et al., 2007). As detailed below, the available microfossil record and the molecular biomarker record suggest that the primary photosynthetic production displayed a large dominance of (cyano)bacteria over eukaryotes, although this view could be biased by the difficulty to identify early eukaryote microfossils and the poor preservation of biomarkers in Paleoproterozoic rocks (Knoll et al., 2007).

2. The Paleoproterozoic microfossil record

Paleoproterozoic rocks are important targets not only for documenting changing redox conditions, but also for micropaleontological investigations. To date, they host the oldest microfossils diagnostic of cyanobacteria (Hofmann, 1976; Knoll and Golubic, 1992) and of eukaryotes (see reviews in Javaux, 2011; Knoll et al., 2006). The Paleoproterozoic record of biological activities (e.g. see below and reviews in Hofmann and Schopf, 1983; Javaux et al., 2012; Knoll, 2003; Schopf, 1992) also includes unidentified microfossils, possible microfossils of iron-oxidizing bacteria, morphologically diverse stromatolites, macroscopic carbonaceous compressions, microbial mat rip-ups, putative fossil or trail impressions, problematic pyritized macrofossils, biological isotopic fractionation of C, S, and N, isotopic fractionation of Fe, and biomarkers. Together, these proxies indicate the presence of eukaryotes, cyanobacteria, green and purple sulfur bacteria, methanogenic archaea and/or bacteria, sulfate-reducing bacteria, methanotrophic bacteria and/or archaea, iron-oxidizing bacteria, anoxygenic photosynthetic bacteria, and denitrifying bacteria (Fig. 1).

2.1. Identifying early microfossils

Microfossils can be made of various altered derivatives of initial biomolecules (e.g. resilient biopolymers such as cell wall polysaccharides), upon which secondary molecules (e.g. derivatives from more labile proteins, lipids) may have grafted during diagenesis (de Leeuw et al., 2006). Some originally organic ultrastructures may be replaced by diagenetic minerals, e.g. by pyrite (Cosmidis et al., 2013; Wacey et al., 2013). Minerals formed in vivo by/on the organism and their diagenetic/metamorphic byproducts may also be associated with microfossils (Crosby et al., 2014; Lepot et al., 2017). Preservation and composition of organic microfossils, of their diagenetic mineral replacements, and of biominerals depend on the original biological composition of the cellular structures (and ultrastructures) and the conditions of preservation, diagenesis, and degree of metamorphism (Alleon et al., 2016a; Alleon et al., 2016b; Schopf et al., 2005). Micro- to nano-scale characterization of organic structures and associated biogenic/diagenetic/metamorphic minerals is required to demonstrate that microfossils are endogenous (i.e. not contaminants), syngenetic (displaying the same age as the rock), and of biogenic morphology (Foucher et al., 2015; Javaux et al., 2012; Laflamme et al., 2011; Lepot, 2011; Oehler, 2014; Wacey et al., 2016). Raman microspectrometry provides information of the organization of aromatic groups in fossil organic matter at the micrometer scale, which is strongly correlated to organic-matter maturity (Schopf et al., 2005); hence, correlation of Raman-derived organic-matter maturity with independent maturity parameters (e.g. mineral assemblages, O-isotopes) provide crucial constraints on the syngenicity of the organic matter (e.g. Alleon et al., 2016b; Javaux et al., 2010). Microscopy is crucial to distinguish i) fossilization of biogenic/anatomical structures, ii) late endolithic contamination (Westall and Folk, 2003) and iii) mineral microstructures associated with migrated organic matter mimicking microfossils (Brasier et al., 2015; Brasier et al., 2005; Lepot et al., 2009b; Van Zuilen et al., 2002). Methods of microscopy include multiplane optical imaging (Brasier et al., 2005), scanning and transmitted electron microscopy on acid-extracted microfossils (Cloud and Hagen, 1965; Javaux et al., 2004; Moczydłowska and Willman, 2009), microscale Raman imaging (Schopf and Kudryavtsev, 2009), Transmission Electron Microscopy performed on Focused Ion Beam sections (Lepot et al., 2017; Moreau and Sharp, 2004; She et al., 2013; Wacey et al., 2012), and nanotomography using Focused Ion Beam ablation coupled to electron microscopy (Wacey et al., 2016). Complex ultrastructures such as trilaminar walls, structured wall reticulation and wall processes (e.g. Javaux et al., 2004; Moczydłowska and Willman, 2009b) represent diagnostic evidence for microfossils that so far have not been reproduced abiotically. When the morphology of putative microfossils is simple, such as spheres and tubular sheaths, microfossil demonstration is more complex. In abiotic mimics, the distribution of organic matter is templated by the host mineral (Buick, 1990). In contrast, in microfossils, the micro/nanostructure of the mineral matrix appears templated by the organic matter and the taphonomic sequence of the microorganism (Kempe et al., 2005; Lekele Baghekema et al., 2017; Lepot et al., 2017; Moreau and Sharp, 2004; Wacey et al., 2012). Microscopy must be complemented by macro-scale characterization of the geological context and of past/recent alteration of the rocks to constrain paleoenvironments, taphonomic (post-mortem) conditions, and possible abiotic processes mimicking microfossils.

Once a microstructure has passed the tests of endogenicity, syngenicity, and biogenicity, the next challenge consists in taxonomic identification. Paleontologists have to rely on information other than the genome and internal cellular organization to identify the biological affinities of early microfossils. Using a combination of morphology and microchemistry may permit differentiation between prokaryote and eukaryote microfossils. Size is not a good criterion to differentiate fossil prokaryotes from eukaryotes since extant pico-eukaryotes (1–2 μm in diameter) and large prokaryotes (such as 100 μm long cyanobacterial akinetes, or bacterial cells such as *Thiomargarita* reaching up to 600 μm in diameter) are documented in nature (see review in Javaux et al., 2003). The analyses of wall ultrastructures may be used for recognition of eukaryotic origin (Arouri et al., 2000; Javaux et al., 2003; Moczydłowska and Willman, 2009; Talyzina and Moczydłowska,

2000b; Willman and Cohen, 2011). Wall ultrastructure (e.g. tri-laminar, or perforated by canals), specific wall ornamentation, and the presence of excystment structures (openings through which cells are released from the cyst) can clarify the eukaryotic affinities of microfossils, sometimes even at the level of specific clades. Excystment structures, if observed in a large population, may be differentiated from occasional tearing, and point to an eukaryotic affinity. However, some cyanobacterial envelopes can reach large sizes (a few tens of micrometers in diameter) and open in a fashion resembling eukaryotic excystments (Waterbury and Stanier, 1978); hence other criteria, such as a complex wall ultrastructure, should be used to confirm a eukaryotic affinity. In contrast, due to their small size and to post-mortem morphological convergence (Schopf, 1975), it is often difficult to provide morphological/ultrastructural constraints on the nature of putative prokaryotic microfossils. Recent studies using transmission electron microscopy or nanotomography have provided new morphological information on the smallest Paleoproterozoic microfossils (Brasier et al., 2015; Lepot et al., 2017; She et al., 2013; Wacey et al., 2012).

Micro-analyses of organic molecules such as micro-FTIR (e.g. Arouri et al., 1999; Marshall et al., 2005; Steemans et al., 2010) and micro-Raman spectroscopy (e.g. Javaux and Marshall, 2006; Marshall et al., 2005) can show inter-specific differences in the functional group signature of single microfossils. For example, FTIR signatures such as abundant long polymethylenic chains point to preservation of algaenan from chlorophyte or eustigmatophyte microalgae (Arouri et al., 1999; Marshall et al., 2005). Nano-analyses of functional groups can be performed using Scanning (transmission) X-ray microscopes (SXM/STXM). STXM revealed the preservation of N- and O-bearing functional groups in Paleoproterozoic microfossils (Alleon et al., 2016b) and SXM revealed S- bearing molecules in Neoproterozoic microfossils (Lemelle et al., 2008). Both N- and S-groups have been proposed as relicts of proteins (Alleon et al., 2016b; Lemelle et al., 2008). However, heteroatoms such as N- and S- may graft diagenetically onto organic matter (Lepot et al., 2009a) and it cannot be confirmed that the former proteins (or other organic precursors) come from the actual microbe precursors to the studied microfossils rather than from ambient soluble molecules. The former hypothesis could be confirmed by demonstration of heterogeneities in N/S/O groups between morphospecies (achieved in Neoproterozoic microfossils using NanoSIMS; Oehler et al., 2006) or between ultrastructures of a single microfossil (achieved with STXM on Phanerozoic fossils; Bernard et al., 2007). In parallel, isotopic microanalyses (House et al., 2000; Lepot et al., 2013; Williford et al., 2013) of organic matter in microfossils reveal inter-specific and/or intra-cellular heterogeneities, indicating that different types of microfossils and/or ultrastructures in a single cell may originate from distinct metabolisms and/or biosynthetic processes. Isotopic microanalyses provided new clues that *Leiosphaerida crassa* and *Myxococcoides* sp. associated in the same Neoproterozoic rock represent algae and cyanobacteria, respectively (Williford et al., 2013). One limitation of this spatially-resolved molecular/isotopic approach is our limited knowledge of the changes occurring to the morphology, ultrastructure and chemistry of extant (micro)organisms during fossilization. This approach thus requires comparative actualistic studies of taphonomic processes affecting diverse organisms in a range of natural and experimental environmental conditions (e.g. Alleon et al., 2016a; Chalansonnet et al., 1988; Javaux and Benzerara, 2009; Kleinteich et al., 2017; Lepot et al., 2014; Li et al., 2013; Picard et al., 2016; Schiffbauer et al., 2012; Storme et al., 2015).

Other important challenges in identifying early microfossils include the limitations of actualism (early microorganisms may not have been ancestors of extant clades but stem clades, and thus not comparable) and the possibility of morphological and chemical convergence between unrelated clades. Even when precise identification failed, fossils document steps in biological and biochemical innovations (Butterfield, 2009; Brasier et al., 2015; Javaux, 2007, 2011; Javaux and Knoll, 2017; Javaux et al., 2001; Knoll et al., 2006). Original biological properties (e.g. morphology, chemistry, division pattern, spatial distribution patterns) may be well preserved, altered or erased by fossilization processes that vary depending on the physico-chemistry of the fossilization environment and the composition of the organism. A good understanding of taphonomic biases is essential for deciphering the original biology.

2.2. Paleoproterozoic eukaryotes

Eukaryotes have developed some fundamental biological innovations since at least the late Paleoproterozoic, such as genetically-programmed excystment structures, reproduction by budding or binary division, multicellularity, and complex ornamentation requiring a sophisticated cytoskeleton and endomembrane system (Javaux and Knoll, 2017; Javaux et al., 2001), and even macroscopic size (Zhu et al., 2016). The molecular clocks are discussed below using the demonstrable, possible and putative records of fossils and biomarkers.

2.2.1. Molecular clues?

Due to contamination and maturity issues, reliable sterane biomarkers for crown-group eukaryotes are only found in Neoproterozoic and younger rocks (Brocks et al., 2008; Brocks et al., 2017; Flannery and George, 2014; French et al., 2015; Knoll et al., 2007; Rasmussen et al., 2008; Summons and Walter, 1990). However, biomarkers indicate the presence of green algae (Brocks et al., 2017) as well as demosponges (Love et al., 2009) and possible toxic protists (Brocks et al., 2016) in the Neoproterozoic, implying an earlier origin of stem and crown-group eukaryotes, as suggested by molecular clocks possibly as early as the Paleoproterozoic GOE (Eme et al., 2014; Gold et al., 2017; Parfrey et al., 2011; and review in Javaux and Knoll, 2017).

2.2.2. Oldest eukaryotic microfossils

The oldest unambiguous eukaryotic microfossils are large (100–300 μm) organic-walled vesicles (acritarchs) ornamented with concentrically striated walls (*Valeria lophostriata*) (Fig. 2a, b). One sphaeromorph from the Changzhougou Fm, China (Fig. 4a in Lamb et al., 2009) shows concentric striations and resembles *Valeria lophostriata*. The Changzhougou Fm, is younger than the 1673 ± 10-Ma U-Pb age of zircons in a granite-porphyry dyke that cuts underlying rocks, and older than the 1625.3 ± 6.2-Ma ash bed in overlying beds (Li et al., 2013). This species also occurs in the overlying ~1.65 Ga Chuanlinggou Formation (Changcheng Supergroup, China) (Lamb et al., 2009; Peng et al., 2009; Zhang, 1986), in the > 1.65-Ga Mallapunyah Formation (McArthur Supergroup, Australia, Fig. 1A 7,8) (Javaux, 2007) and in many younger Proterozoic siliciclastic successions. Rhythmic ridge patterns at the surface of *Valeria lophostriata* have been suggested to represent an in vivo growth pattern (Pang et al., 2015) or a taphonomic pattern (Hofmann, 1999). These striations are in fact wall ornamentations, as shown by scanning Electron Microscopy (SEM) images evidencing that they are 1-μm-spaced ridges located on the inner side of the vesicle and not taphonomic features (Javaux et al., 2004). B-Z-type reactions or Turing reaction-diffusion processes may have formed the striations in vivo, possibly as a mechanism to guide biologically programmed excystment through medial split (Pang et al., 2015) although medial split is known in many other unornamented and ornamented vesicles. These spheroidal fossils often show excystment structure by medial split, with the separated half-vesicles usually rolling up over themselves (Fig. 2b).

2.2.3. Eukaryotic microfossil diversification

Recently, the age of a moderately diverse microfossil assemblage from the Beidajan Formation in the Ruyang Group, in China, first dated to about 1.3 Ga (Xiao et al., 1997), has been revised to the late Paleoproterozoic–early Mesoproterozoic (Pang et al., 2013). Detrital zircons indicate that Ruyang deposition began no earlier than 1744 ± 22 Ma (Hu et al., 2014), and xenotime Pb-Pb ages of about 1411 ± 27 Ma for the overlying Luoyu Group constrain deposition from above (Lan et al.,

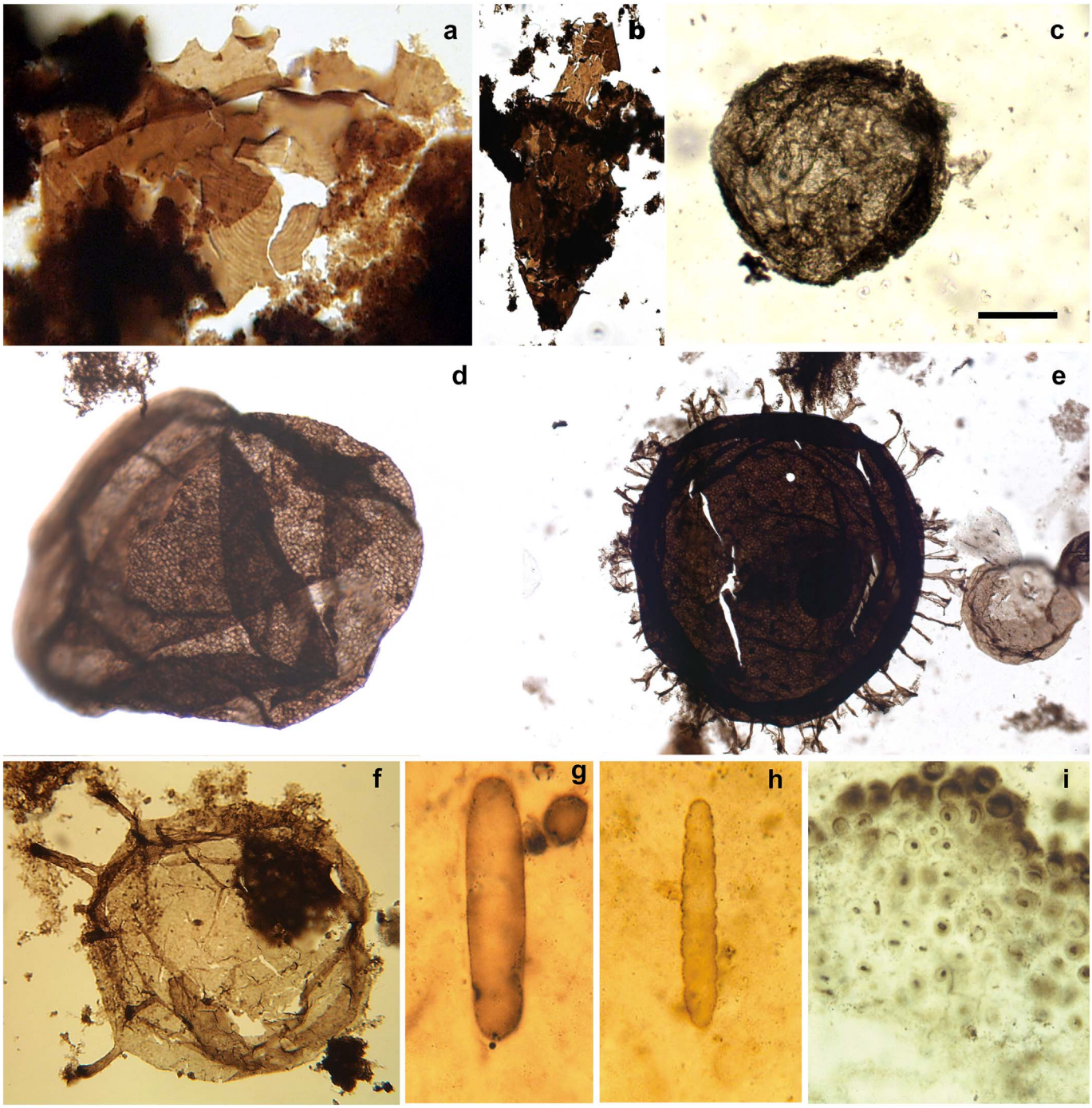

Fig. 2. Paleoproterozoic microfossils: eukaryotes, sphaeromorphs and cyanobacteria.
a, b. *Valeria lophostriata*, > 1.65 Ga Mallapunyah Fm, Australia, an early eukaryote with a wall ornamented with concentric striations.
c. *Leisphaeridia sp.*, a sphaeromorph from the 1.9 Ga Kondopoga Fm, Karelia, Russia. Scale bar in c = 100 μm for b, c, e, 50 μm for a, d, f.
d. *Dictyosphaera delicata*, a protist from the 1.7 to 1.4 Ga Ruyang Group, China.
e. *Shuiyousphaeridim macroreticulatum* (left), a protist, and *Leiosphaeridia minutissima*, a sphaeromorph from the 1.7 to 1.4 Ga Ruyang Group, China.
f. *Tappania plana*, a protist from the 1.5 Ga Roper Group, Australia.
g. *Archaeoellipsoides*, interpreted as possible cyanobacteria akinetes, Mesoproterozoic Billyakh group, Siberia. This specimen is 80 μm long (photo courtesy of AH Knoll).
h. Cyanobacteria trichome, Mesoproterozoic Billyakh Group, Siberia. This specimen is 85 μm long (photo courtesy of AH Knoll).
i. *Eoentophysalis*, cyanobacterial colonies from silicified stromatolites, 1.9 Ga Belcher Group, Belcher Islands, Canada. Ellipsoidal envelopes around cells are 6–10 μm in diameter (photo courtesy of A.H. Knoll).

2014). A U-Pb zircon date from an ash bed within the Luoyu Group potentially constrains Ruyang deposition to be older than 1611 ± 8 Ma, but the abundance of detrital grains in the dated bed and the wide range of ages for individual zircons (Su et al., 2012) suggest that the published date may provide only a maximum age constraint on Luoyu deposition (Lan et al., 2014). This 1744 ± 22 to 1411 ± 27 Ma assemblage includes sphaeromorphs, large filaments, segmented oval vesicles, but also unambiguous eukaryotes such as the *Valeria lophostriata* described above, and *Dictyosphaera delicata* ornamented with a reticulated wall and showing a circular excystment

structure (pylome). Acanthomorph (process-bearing) acritarchs include: the complex acanthomorph acritarch *Tappania plana* bearing heteromorphic processes and neck-like extensions, and showing evidence of budding, a large acanthomorph densely covered with small processes (*Gigantosphaeridium fibratum*), and *Shuiyousphaeridium macroreticulatum* (Fig. 2e), another complex acritarch of the assemblage, bearing furcated processes and a multilayered wall made of imbricated polygonal organic plates (Agić et al., 2015; Javaux et al., 2001; Javaux et al., 2004; Schiffbauer and Xiao, 2009; Yin, 1997; Yin et al., 2005). *Tappania plana* is also reported in the 1.45 Ga Roper Group, Australia (Javaux and Knoll, 2017; Javaux et al., 2001) (Fig. 2f), in the 1.45 Ga Lower Belt Group, Montana (Adam et al., 2017), the ~1.3 Ga Kamo Gp, Siberia (Nagovitsin et al., 2010), the Sarda Formation of the Bahraich Group, Ganga Basin (Prasad and Asher, 2001), and possibly in correlative beds of the Kheinjua Group, Vindhyan Basin (Prasad et al., 2005) in northern India. U-Pb zircon dating of ash beds from the Deonar "Porcellanite" Formation just below the Vindhyan succession containing unambiguous *Tappania* indicates that these fossils are ≤1631 ± 1 Ma old (Ray et al., 2002). This also constrains the age of morphologically complex acritarchs including acanthomorphs (*Shuiyousphaeridium echinulatum, Cymatiosphaeroides kullingii)* reported from the overlying Chitrakoot Formation, Semri Group, Vindhyan Supergroup, India (Sharma et al., 2016; Singh and Sharma, 2014) although ages up to 1.650 ± 89 Ga have been reported (Bengtson et al., 2009). Some Paleoproterozoic microfossils have been interpreted as possible green algae based on morphological comparison with modern algae (Moczydłowska et al., 2011; Agić et al., 2015). These interpretations remain to be confirmed by other types of analyzes, because of the possibility of morphological convergence (Knoll, 2014).

2.2.4. Other possible eukaryote microfossils

In the absence of wall ornamentation, as explained above, detailed studies of the wall ultrastructure may permit the identification of eukaryotic microfossils in some cases (Cohen et al., 2009; Javaux et al., 2003; Javaux et al., 2004; Javaux and Marshall, 2006; Moczydłowska and Willman, 2009b; Talyzina and Moczydłowska, 2000a), especially when ultrastructure analyses are combined with wall chemistry (Javaux et al., 2003; Javaux et al., 2004; Javaux and Marshall, 2006; Marshall et al., 2005). In Paleoproterozoic and younger rocks, large, smooth organic-walled vesicles (up to a few 100 μm unornamented acritarchs, also called leiospheres or sphaeromorphs) are common and may display a medial split, but the absence of any wall ornamentation prevents their attribution to the eukaryotic domain. They could represent early protists or large envelopes of prokaryotes such as those of some cyanobacteria, which can open in a fashion that could be confused with a eukaryotic medial split (Waterbury and Stanier, 1978). Large sphaeromorphs also occur in the Mesoarchean (Javaux et al., 2010) but do not show medial split or complex wall ultrastructure and cannot be related to a particular clade or domain. Multilayered wall ultrastructures and medial splits were reported in 1.8 Ga old large Changcheng sphaeromorphs, possibly relating those to early eukaryotes (Lamb et al., 2009; Peng et al., 2009). Rare large (up to > 300 μm) carbonaceous vesicles (acritarchs) and fragments of organic sheaths of unknown biological affinities also occur in siltstones from the upper members of the ~1.9 Ga Kondopoga Formation, Karelia, Russia (Javaux et al., 2012) (Fig. 2c). Poorly preserved ambiguous acritarchs from Karelia were first mentioned by (Timofeev, 1982). Sphaeromorphs have also been reported in siltstones and silty black shales from the FB2 subunit of the the ~2.1 Ga old Francevillian Group of Gabon (El Albani et al., 2014). Large spheroidal unicells from 2.1–1.88 Ga stromatolitic cherts of the Vempalle Formation, India (revised age in Chakrabarti et al., 2014) have also been suggested as putative eukaryotes (Schopf and Prasad, 1978), however size alone is not a sufficient criteria and other analyses are necessary to confirm this hypothesis (see Section 2.1).

2.2.5. Putative multicellular eukaryotes

Recently, phosphatized microfossils from the ~1.6 Ga Chitrakoot Formation have been interpreted as possible crown-group red algae (Bengtson et al., 2017), based on putative pyrenoids preserved in large tubes *Rafatazmia* and on multicellular thallus-like *Ramathallus* showing possible cellular differentiation. If the age and affinity of these microfossils are confirmed, they would evidence the acquisition of the chloroplast by eukaryotes 500 Myr earlier than evidenced by the 1.1 Ga red algae *Bangiomorpha* (Butterfield, 2000). Recent molecular clock studies suggest an origin of the common ancestor of the *Archaeplastida* (red, green and Glaucophyte algae) around 2.1–1.6 Ga but crown groups originated later between 1.3 and 0.9 Ga (Sánchez-Baracaldo et al., 2017). Branching and/or fibrous structures reported in ~2.8–2.7 Ga lacustrine rocks have been proposed as fossils of early algae (Kaźmierczak et al., 2016). However, we interpreted these Archean microstructures as altered and metamorphosed biotite crystals, which commonly display similar microstructures and chemical compositions (Morad, 1990). The carbonaceous particles detected by Kaźmierczak et al. (2016) in these fibrous/branching clays may represent amorphous kerogen commonly embedded in Archean clays (Lepot et al., 2009a). Finally, the palynological extract of Kaźmierczak et al. (2016) is transparent, and likely represents a preparation contaminant or a mineral rather than black and opaque Archean (i.e. metamorphic) organic matter.

2.2.6. Possible macrofossils

Other possible Paleoproterozoic eukaryotes include macroscopic carbonaceous compressions and trace fossils. Centimetric carbonaceous compressions preserved on bedding plane surfaces include spherical *Chuaria*, sausage-shaped *Tawuia* and coiled filamentous *Grypania* (Xiao and Dong, 2006). *Grypania spiralis* from the 1.87 Ga Negaunee Iron Formation, Michigan (Han and Runnegar, 1992; redated by Schneider et al., 2002) is ~1 mm in diameter, up to 90 mm in length, and forms coils with a diameter up to 30 mm across. Samuelsson and Butterfield (2001) have questioned the eukaryotic nature of these earlier structures from Michigan, while observations by Knoll (in Knoll et al., 2006) suggest that it was an organism, and not a colony or composite of much smaller prokaryotic filaments. Younger forms also called *Grypania spiralis* from the ~1.45 Ga Vindhyan Supergroup, India, are septate and much longer (about 500 mm), and are more convincingly eukaryotic. Reassessment of Paleo- and Mesoproterozoic, macroscopic, coiled filamentous compressions suggests a cyanobacterial affinity for some of them, while others might be dubiofossils and 'tissue-grade organisms' (Sharma and Shukla, 2009) or macroalgae (Xiao and Dong, 2006). Morphometric studies combined with the detection of highly aliphatic organic matter have been interpreted as a possible algal affinity (Sharma et al., 2009), however, an aliphatisation process during diagenesis is also possible (de Leeuw et al., 2006), and the *Chuaria* wall biopolymer also contain aromatic moieties (linked or not to the maturity of the biopolymer). Tang et al. (2017) recently suggested that Tonian specimens of *Chuaria* represent multicellular vegetative stage rather than an inert cyst. Carbonaceous compressions with linear to lanceolate shapes up to 30 cm long and with an attachment structure have been reported in the earliest Mesoproterozoic, 1.56 Ga old Gaoyuzhuang Formation in North China (Zhu et al., 2016). Their large size and complexity indicate the evolution of benthic macroscopic eukaryotes; however they are not preserved in situ and their algal or other affinity is unknown.

2.3. Cyanobacteria

2.3.1. Oscillatoriales-like filaments

Broad (15–25 μm) filaments of *Syphonophycus transvaalensis* in the latest Archean 2.52 Ga Gamohaan Formation of South Africa probably represent non-heterocystous cyanobacteria similar to modern Oscillatoriales (Klein et al., 1987). This is supported in particular by their thick (~2 μm) sheath that is common in cyanobacteria but not in other types of bacteria reviewed in Lekele Baghekema et al. (2017) and their alternating vertical and horizontal disposition in mats (Butterfield, 2015b; Knoll and Golubic, 1992). However, it is possible that thick sheaths may also have occurred in non-cyanobacterial bacteria in the past, in which case additional morphological/microchemical criteria supporting cyanobacteria would be necessary. Similar Oscillatoriales-like microfossils occur in the 2.1–1.88 Ga (Chakrabarti et al., 2014) stromatolitic cherts of the Vempalle Formation, India (Schopf and Prasad, 1978). Moreover, the 1.62 Ga Dahongyu Formation also hosts broad (25–36 μm in diameter) filaments with barrel-shaped cells named *Oscillatoriopsis*; these have been interpreted as oscillatoriales cyanobacteria (Shi et al., 2017), although Knoll et al. (1988) proposed that similar *Oscillatoriopsis* of the ~1.8 Ga Duck Creek Formation could represent S-oxidizing bacteria (*Beggiatoa*) as well.

2.3.2. Archaeoellipsoides

Sausage-shaped vesicles (*Archaeoellipsoides,* Fig. 2g) interpreted as putative akinetes (resting cysts) of nostocales cyanobacteria occur in the 2.1 Ga Francevillian Series in Gabon (Amard and Bertrand Sarfati, 1997). These may represent some of the oldest remains of cyanobacterial cells, although their small size (usually < 5 μm in diameter) and morphological similarity to unicellular fossil (cyano)bacteria make their akinete origin uncertain (Butterfield, 2015b). Sausage-shaped microfossils with larger diameter (~10–30 μm) occurring in cherts from the 1.65 Ga McArthur Group have been more confidently attributed to cyanobacterial akinetes (Tomitani et al., 2006). However, the fact that other microorganisms such as giant bacteria and green algae may display the same morphology and that these putative Proterozoic akinetes have not been found attached as part of trichomes of cells has led to question this attribution (Butterfield, 2015b). Importantly, the modern akinete-forming cyanobacteria are also the only cyanobacterial group that form specialized cells (heterocysts) enabling aerobic N_2-fixation. These akinete-forming filamentous cyanobacteria perform oxygenic photosynthesis in oxygenated, planktonic to continental (freshwater, sometimes soil/rock surface) habitats (Golubic and Seong-Joo, 1999). If confirmed, Proterozoic akinetes in marine deposits may represent planktonic heterocystous cyanobacteria. In turn, inferring their ability to fix N_2 in oxygenated environments (Tomitani et al., 2006) requires the assumption that ancient akinete-forming cyanobacteria were also capable of forming N-fixing heterocysts like their modern counterparts (Butterfield, 2015b).

2.3.3. Coccoidal/unicellular cyanobacteria

The picoplanktonic cyanobacteria that dominate today's marine cyanobacterial primary production have not been found in the Proterozoic fossil record, possibly due to their dominantly simple unicellular spheroidal morphologies or preservation bias (Golubic and Seong-Joo, 1999). In contrast, benthic colonies of coccoidal (spheroidal) microfossils of the Paleoproterozoic include the oldest unambiguously identified microfossils of cyanobacteria. Among these, *Eoentophysalis belcherensis* (Fig. 2i) of the 1.9 Ga Belcher Group, from the Belcher Islands, Canada (Hofmann, 1976), are the oldest undisputed cyanobacteria. The Belcher Group succession comprises chert lenses and nodules in silicified stromatolites grown in tidal and shallow subtidal waters on a carbonate platform (Golubic and Hofmann, 1976; Hofmann, 1976). The cherts contain three-dimensionally preserved filamentous and coccoidal (spheroidal) microfossils, including fossilized colonies of microscopic cells displaying superficial darkening suggested as the result of pigmentation. The distribution and pattern of division of these later microfossils (*Eoentophysalis belcherensis*), colonies of coccoidal cells dividing by binary fission in three planes inside preserved external envelopes and darker (possibly desiccated or pigmented) colony surfaces, permit relating them to the living genera of cyanobacteria *Entophysalis* (Golubic and Hofmann, 1976; Hofmann, 1976). *Eoentophysalis* (Fig. 2i) has been recorded in other Paleoproterozoic and younger successions (Knoll and Golubic, 1992).

At the end of the Paleoproterozoic, the 1.62 Ga Dahongyu Formation of northern China displays additional morphospecies diagnostic of cyanobacteria. These include endolithic colonies forming pseudofilaments interpreted as fossil counterparts to the extant hyellacean (pleurocapsales) cyanobacteria (Zhang and Golubic, 1987). These also include the coccoid morphosphecies *Gloeodiniopsis* sp. interpreted as chroococcales cyanobacteria based on large (19–68 μm), thin and occasionally multi-layered wall, thin and ghost-like outer sheath, division pattern in single envelope and envelope splitting pattern (Shi et al., 2017). Other possible chroococcales cyanobacteria (*Gloeocapsomorpha*) have been reported in the underlying 1.68–1.62 Ga Chuanlinggou Formation (Timofeev, 1966, reviewed in Mendelson and Schopf, 1992, but we could not access this publication in Russian for verification).

2.3.4. Cyanobacterial diversification?

These Paleoproterozoic cyanobacteria may represent the onset of an important diversification in (identified) cyanobacteria occurring soon after in the Mesoproterozoic as attested for example by microfossils (e.g. Fig. 2h) of Siberia (Sergeev et al., 2002). However, a number of unidentified microfossils in Paleoproterozoic rocks may represent a hidden diversity among cyanobacteria, as discussed below.

2.4. Gunflint-type microfossil assemblages

Gunflint-type microfossil assemblages occur in shallow water (stromatolitic and oncoid-rich) cherts and non-stromatolitic cherts (possibly of relatively deeper water). The type and best preserved assemblage was found in the 1.88 Ga Gunflint Iron Formation, Canada (Alleon et al., 2016b; Awramik and Barghoorn, 1977; Barghoorn and Tyler, 1965; Fralick et al., 2002). The Gunflint-type microfossil assemblage is usually defined by the association of its dominant microfossils (Fig. 3) including: 1) filaments (*Gunflintia* and other undetermined filaments that could represent cyanobacteria, or Fe −/S-oxidizing bacteria; Barghoorn and Tyler, 1965; Cloud, 1965; Knoll et al., 1988), 2) *Huroniospora* (cyanobacteria or other microorganisms, possibly heterotrophs: Barghoorn and Tyler, 1965; Strother and Tobin, 1987), 3) *Eoastrion* (Fe-/Mn-oxidizing bacteria or dubiofossils: Cloud, 1965; Krumbein, 2010) and 4) *Kakabekia* (possibly ammonia-metabolizing bacteria: Siegel and Siegel, 1970). These assemblages may hold key information on the Paleoproterozoic biosphere. Indeed, they are absent in older rocks and scarce in younger rocks, but widespread in the Paleoproterozoic, including occurrences in:

the 2.1 Ga Francevillian cherts of Gabon (Amard and Bertrand Sarfati, 1997), the 1.88 Ga Ferriman Group of Canada (Edwards et al., 2012; Knoll and Simonson, 1981), the 1.8 Ga Tyler Formation of Michigan (Cloud and Morrison, 1980), the 1.88 Ga Frere Formation, Australia (Rasmussen et al., 2012; Walter et al., 1976b), the 1.8–1.65 Ga McArthur Group, Australia (Muir, 1983; Oehler, 1977), and the 1.77–1.65 Ga Dahongyu Formation (Yun, 1984).

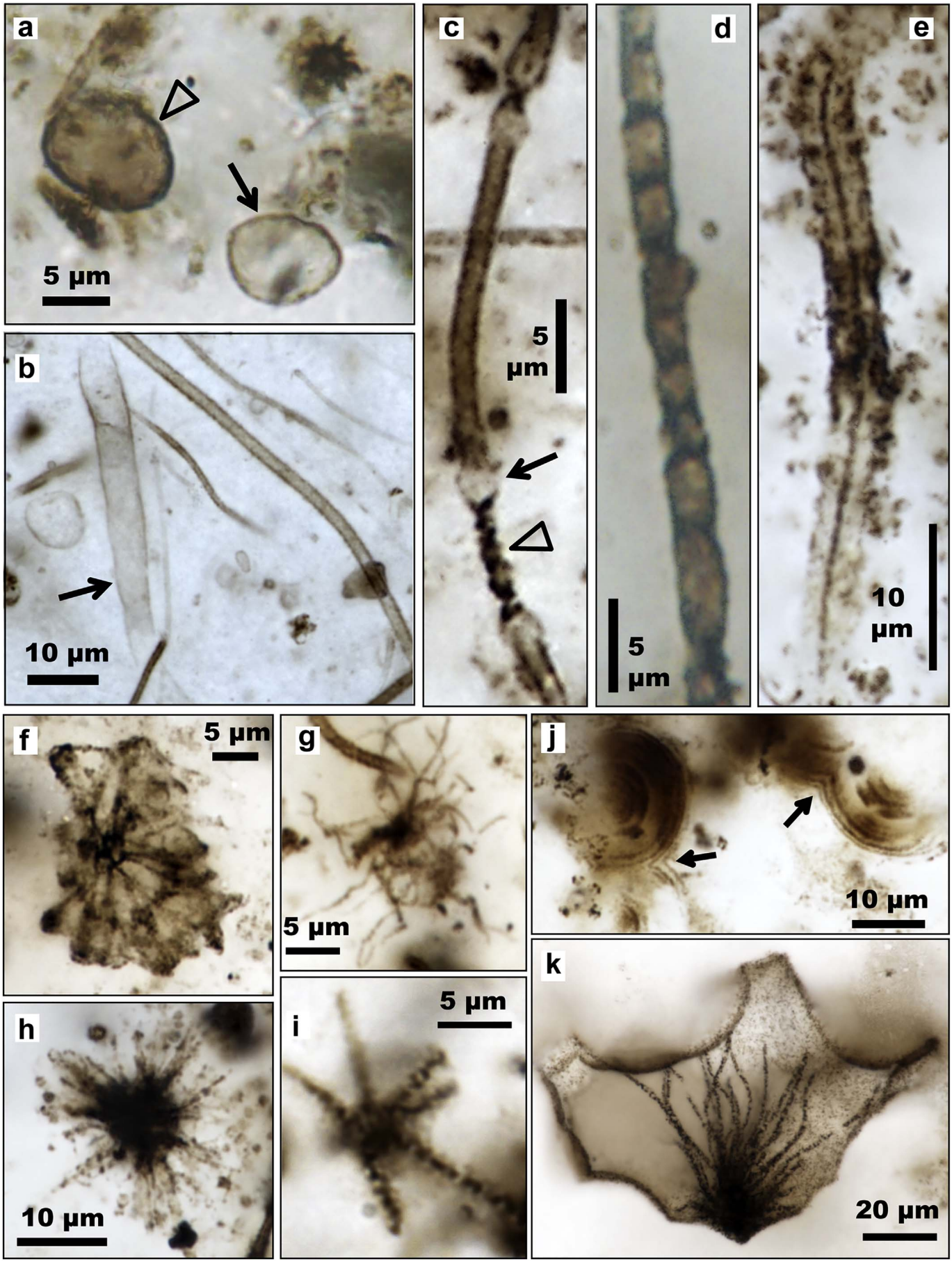

(caption on next page)

Fig. 3. Microfossils from a stromatolite of the Gunflint Iron Formation. Multiplane photomicrographs taken with 100 × objectives (NA = 0.9) and produced by combination of images recorded at multiple focal depths. Microscopes: Olympus BX60 (a, d, i), Nikon Ni-E (all others). a. Thick-walled *Huroniospora* (arrowhead) are distinguished by a dark black organic wall creating an opaque microstructure. Thin-walled *Huroniospora* (arrow) in contrast appear completely transparent. b. Sheaths of filamentous microfossils. Type 1 *Gunflintia minuta* includes the narrower empty sheaths, whereas *Animikiea* (arrowed) includes empty sheaths broader than ~3 μm. c. Locally degraded sheath of Type 1 *Gunflintia minuta* displaying regions depleted in organic matter (arrow) and constricted regions with granularization of organic matter (arrowhead). d. Type 2 *Gunflintia minuta* with cell-like segmentation. e. Unnamed filament with central carbonaceous canal. f. *Kakabekia*, an umbrella-shaped microfossil. g-i. Various *Eoastrion*, a group of star-shaped microfossils. j. Quartz with concentric zones coated by organic matter. Hemispherical structure and sphere coalescence (arrows) argue for an abiotic (botryoidal) growth. k. Filamentous, star-shaped organic microstructure in a void now cemented by quartz (sample top direction is on the left).

The problematic nature of microfossils in Gunflint-type assemblages are discussed below.

2.4.1. Cyanobacteria

Animikiea septata consists of sheaths 7–10 μm wide with surface striations similar to those formed by barrel-shaped cells (Awramik and Barghoorn, 1977; Barghoorn and Tyler, 1965) that could represent cyanobacteria as well as S-oxidizing Beggiatoa (Knoll et al., 1988). *Megalytrum diacenum* (Knoll et al., 1978) and *Corymbococcus hodgkissii* (Awramik and Barghoorn, 1977) consist of multiple cells embedded in a common spheroidal sheath consistent with chroococcales or other colonial bacteria. All these likely cyanobacterial microfossils are scarce and dispersed and may be allochthonous (Knoll et al., 1988; Strother and Tobin, 1987).

2.4.2. Eosphaera and Leptotrichos: possible eukaryotes?

Eosphaera tylerii in the Gunflint Iron Formation consists of spheres ~30 μm in diameter displaying a thin outer wall and a thicker inner wall (Barghoorn and Tyler, 1965; Brasier et al., 2015). The space between these concentric walls is interspersed with sub-spherical vesicles 1–7 μm in diameter. An assignment to red algae (Tappan, 1976) has been refuted by Awramik and Barghoorn (1977). An assignment to volvocacean green algae has been proposed (Kaźmierczak, 1979), though contested by Brasier et al. (2015) on the basis that they miss an internal sphere. This question should be addressed with comparative nanostructural studies such as those performed by Brasier et al. (2015) on Devonian putative volvolcacean microfossils (Kaźmierczak, 1979) and on artificial volvocacean fossils, but also by microchemical analyses. Alternatively, Brasier et al. (2015) proposed that *Eosphaera* could represent a symbiotic consortium. Abundant siderite microspheres found in banded iron formations (BIFs) have been proposed as siderite-replaced *Eosphaera* (Kaźmierczak, 1979), but these microstructures can also form abiotically (Koëhler et al., 2013).

Leptotrichos occurs in non-stromatolitic (Knoll et al., 1978) and flat stromatolitic (Yun, 1984) facies. It consists in 5–30 μm solitary coccoids with internal organic granules that may represent the remains of eukaryotic intracellular ultrastructures or a (cyano)bacterial degradation pattern (Knoll et al., 1978; Williford et al., 2013).

2.4.3. Gunflintia minuta

G. minuta are filaments less than ~3 μm in diameter and several hundred micrometers in length (Fig. 3a-d). *G. minuta* "Type 1" (Lepot et al., 2017) are empty tubes (Fig. 3b), interpreted as fossils of polysaccharide sheaths empty of their trichomes (chains) of cells (Barghoorn and Tyler, 1965). "Type 2" *G. minuta* (Lepot et al., 2017) are chains of rod-shaped quartz grains coated with organic matter (Fig. 3d) that could correspond to trichomes (Awramik and Barghoorn, 1977; Licari and Cloud, 1968) or to a taphonomic alteration of Type 1 *G. minuta* (Brasier et al., 2015). However, the locally degraded Type 1 *G. minuta* only show depletion, constriction and granularization of organic matter but not cell-like structures (Fig. 3c), and Type 2 filaments display a sharp distribution of average segment length (~3.5 μm) consistent with rod-shaped cells (Lepot et al., 2017). The filament curvature has been compared to those of various modern cyanobacteria (Boal and Ng, 2010). Similar mechanistic studies in non-cyanobacterial filamentous bacteria are necessary to use curvature as a potential taxonomic constraint.

2.4.4. Other filaments

Diverse filamentous forms occur as uncommon to rare microfossils in Gunflint-type assemblages. *Animikiea* has been used to regroup the uncommon, thin empty sheaths broader than ~3 μm (Fig. 3b); this microfossil type is morphologically equivalent to *Siphonophycus* microfossils observed in Paleoproterozoic and younger rocks (Schopf, 1992). Accordingly, we suggest synonymization of the trichome-free *Animikiea* as *Siphonophycus* pending comparison of sheath thicknesses with TEM. Even less common are *Animikiea*-like microfossils displaying an organic-rich narrow central canal (Fig. 3e) that could possibly represent degraded cellular content or the inner boundary of a sheath several micrometers thick. *Archaeorestis* comprises enigmatic tubular forms with cyst-like internal spherical structures (Barghoorn and Tyler, 1965). *Gunflintia grandis* is a segmented filamentous microfossil, with cellular structures 4 μm or more in diameter and a much smaller length/diameter ratio than *G. minuta* cells (Barghoorn and Tyler, 1965; Lepot et al., 2017). Filaments ~5 in diameter with a thick (~2 μm) organic sheath and narrow (~1 μm) central canal from the Gunflint-type assemblage of Gabon suggest (c.f. Section 2.3.1) cyanobacteria (Lekele Baghekema et al., 2017).

2.4.5. Huroniospora

Huroniospora is a genus that comprises all the simple smooth-walled spheres 1–16 μm in diameter (Lanier, 1989; Strother and Tobin, 1987), excluding the more complex spheres listed in Sections 2.4.1 and 2.4.2. Microscopy (Fig. 3a) and TEM distinguished thick- (110–600 nm) and thin- (40–60 nm) walled *Huroniospora* (Lepot et al., 2017). Regular reticulation has been used to distinguish the morphospecies *Huroniospora macroreticulata* (Barghoorn and Tyler, 1965; Moreau and Sharp, 2004) and structures evoking cell appendages, budding, reticulation or cell opening have been used to argue against a cyanobacterial origin (Strother and Tobin, 1987). However, TEM revealed that all these wall textures result of the growth of quartz crystals in or through the cell wall (Lekele Baghekema et al., 2017; Lepot et al., 2017; Wacey et al., 2012).

2.4.6. Kakabekia and Eoastrion

Kakabekia umbellata is a rare umbrella-shaped microfossil (Fig. 3f) that resembles an extant microorganism for which in vitro studies suggest the use of ammonia as energy source (Siegel and Siegel, 1970). In our view, up-to-date molecular, metabolic and ultrastructural characterization (as well as naming) of this possible recent counterpart on new cultures/isolates appears necessary to support this comparison. *Eoastrion* comprises uncommon to abundant radiate (star-shaped) structures that resemble micro-colonies of *Metallogenium,* a Mn- and Fe-oxidizing bacterium (Cloud, 1965). However, the highly diverse morphology of *Eoastrion* (Fig. 3g-i) could also be explained by taphonomic processes (Krumbein, 2010) or migration of organic matter, as discussed below.

2.4.7. Abiotic microfossil mimics

The simple shape of putative Archean microfossils is considered problematic (Brasier et al., 2005; Buick, 1990; Knoll et al., 2016). Common minerals, including silica, may form abiotic structures such as tubes, spheres, stars, and spirals (García Ruiz et al., 2002; Livage, 2009) that could drape in bitumen to mimic microfossils. Gunflint-type microfossils have been used as a reference for the identification of

microfossils in older rocks, but their simple morphologies could also possibly be reproduced abiotically. Recent experiments have shown that organic molecules may assemble into tubular and spherical structures during crystallization of elemental sulfur (Cosmidis and Templeton, 2016). However, several features argue that Gunflint-type assemblages hold at least some true microfossils. First, the complex microstructures of the scarce septate filaments and chroococcales-like microfossils with cell division patterns (Awramik and Barghoorn, 1977; Knoll et al., 1978; Lanier, 1989) and the cellular microstructure of Type 2 *G. minuta* have yet to be reproduced with abiotic experiments. Moreover, the micro/nanostructure of quartz grains in *Gunflintia* and *Huroniospora* suggests that silicification was templated by organic microstructures rather than the contrary (Lekele Baghekema et al., 2017; Lepot et al., 2017; Moreau and Sharp, 2004; Wacey et al., 2012). Second, the distribution of *G. minuta* and *Huroniospora* in Gunflint stromatolites displays some patterns that have not been, to our knowledge, reproduced by in vitro growth of abiotic mineral templates. *G. minuta* sometimes occurs as filament bundles wrapping sand grains (Lanier, 1989) similar to filamentous phototrophs in modern stromatolites (Reid et al., 2000). *Huroniospora* sometimes occurs inside granular microstructures (Lanier, 1989) similar to endolithic cyanobacteria of the same modern stromatolites (Stolz et al., 2001). Finally, the preservation of Gunflint-type microfossils upon acid demineralization of the rocks (Cloud and Hagen, 1965; Lekele Baghekema et al., 2017) argue for preservation of resilient biopolymers and morphologies.

Nevertheless, all rocks hosting Gunflint-type microfossils have been thermally altered at least into the stage of oil window (Alleon et al., 2016b; Lekele Baghekema et al., 2017; Schopf et al., 2005) and bitumen could have migrated. Indeed, Gunflint stromatolites locally show concentric zonations of organic matter in botryoidal quartz (Fig. 3j) that most likely formed by displacement of organic matter on growth zones of opal/quartz spheres (Brasier et al., 2005; Buick, 1990; Oehler, 1976). Gunflint stromatolites display void-filling quartz with radiating organic structures (Fig. 3k) closely resembling some *Eoastrion* (Fig. 3i). *Eoastrion* and void-filling radial structures could have formed through radial migration of organic matter. Radial migration of organic matter during silicification experiments (Fig. 5J in Oehler, 1976) created structures similar to some Gunflint Fm dubiofossils (Fig. 1 of Tyler and Barghoorn, 1954). Nanoscale investigation of Francevillian (~2.1 Ga) *Eoastrion* found no diagnostic cellular ultrastructure and revealed radial branches that cut across chlorite crystals suggesting organic matter migration (Lekele Baghekema et al., 2017).

Altogether, the conclusion that cyanobacteria-like microstructures as well as *Gunflintia* and *Huroniospora* are true microfossils is supported by micro/nanostructures and ecological distribution in stromatolites. Such evidences have, so far, been lacking for *Eoastrion* and *Kakabekia*.

2.4.8. Fe-mineralization

Gunflint-type microfossils are commonly pyritized, i.e. their organic matter is replaced by pyrite with preservation of the general morphology with C and N remnants confirming the microfossil precursors (Wacey et al., 2013). Thin- and thick-walled pyritic *Huroniospora* (Lepot et al., 2017; Fig. 4a–c) suggests that pyrite replacement may preserve the original thickness of the precursor organic wall. S-isotope microanalyses showed that pyritization has proceeded through bacterial sulfate-reduction (Wacey et al., 2013). Small hollow pyritic vesicles interpreted as microfossils of heterotrophic sulfate-reducing bacteria occur attached to the pyritized microfossils upon which they could have fed (Wacey et al., 2013). Siderite is also sometimes associated with pyrite (Fig. 4a–c), suggesting that siderite may also replace organic matter through microbial and/or thermal iron reduction (e.g. Fadel et al., 2017).

Iron oxides (Fe_2O_3 and Fe_3O_4) are often associated with microfossils in Gunflint-type assemblages. Cloud (1965) proposed that they could result of microbial Fe-oxidation based on the morphological similarity between Type 1 *G. minuta* and the Fe-oxidizing chemotrophic *Leptothrix*. Fe isotope ratios are consistent with Fe-oxidation by chemotrophic bacteria, cyanobacteria, or abiotic reactions (Mulholland et al., 2015; Planavsky et al., 2009). Trace-element patterns suggest microaerophilic/anaerobic conditions in the Gunflint Formation stromatolites, hence suggesting Fe-oxidizing chemotrophs (Planavsky et al., 2009). However, these patterns may reflect diagenesis rather than seawater compositions (Petrash et al., 2016). Alternatively, Fe-rich groundwater may have encrusted these microfossils in iron post mortem (Shapiro and Konhauser, 2015), although Fe-isotopes support Fe-deposition from seawater (Planavsky et al., 2009). Pyrite- or siderite-replaced microfossils (Fadel et al., 2017; Wacey et al., 2013) may also oxidize/weather into such iron oxide-rich, organic-poor microfossils (Licari and Cloud, 1972; Shapiro and Konhauser, 2015).

In a Gunflint Formation stromatolite preserved of groundwater oxidation, Fe^{2+}-minerals (pyrite, siderite and greenalite) were systematically observed within thick-walled *Huroniospora* (Fig. 4d), Type 2 *G. minuta*, and *Gunflintia grandis,* but absent in *Animikiea*, Type 1 *G. minuta* and thin-walled *Huroniospora* (Lepot et al., 2017). Francevillian thick-walled *Huroniospora* displayed a similar relationship with Fe-minerals (Lekele Baghekema et al., 2017). The morphospecies-specific and

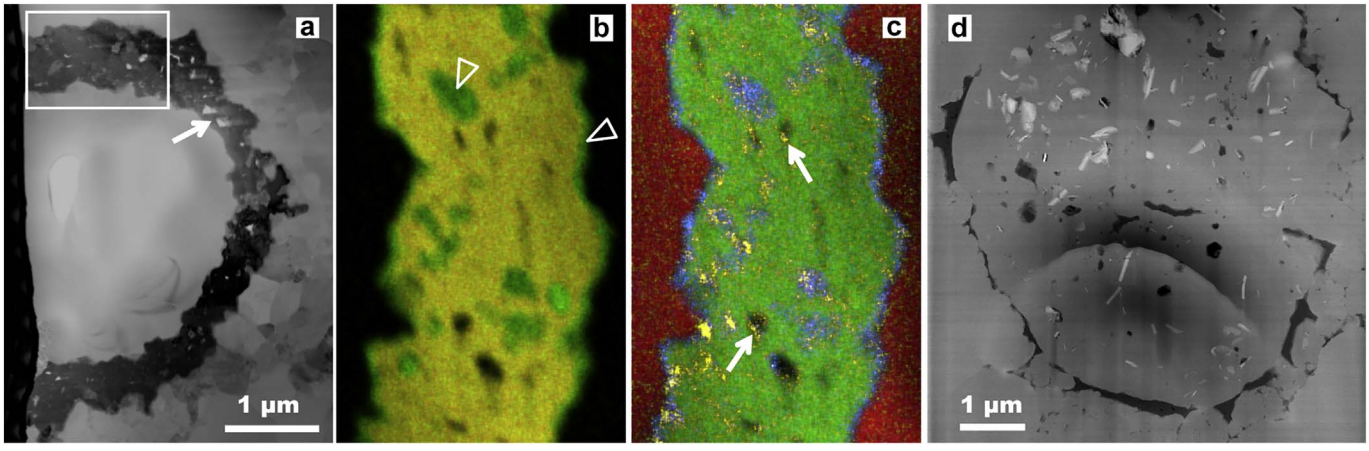

Fig. 4. Fe-minerals associated with *Huroniospora*. Scanning transmission electron microscope images of Focused Ion Beam ultrathin sections. a. Bright field image of the wall of a *Huroniospora* replaced by porous (arrow) pyrite (in black). b–c. STEM-EDXS (13 nm probe) elemental maps of the boxed region in (a). Pyrite [Fe + S: yellow in (b), Fe: green in (c)] comprises most of the mineralized wall structure, while Ca-rich siderite [$Fe_{0.92}Ca_{0.08}CO_3$; Fe without S: green in (b) and Ca: blue in (c)] occurs at the margins and inside some pores of the pyritic wall. Some pores are empty (black), while others are partly filled with organic C [yellow in (c), possibly epoxy contamination]. Quartz [Si in red in (c)] is found inside and outstide the fossil. d. Dark-field image of a *Huroniospora* displaying thick organic walls (in black) in quartz (grey). Abundant Fe-minerals (Ca-poor siderite and greenalite, in white) occur inside this microfossil. Panel (d) reproduced from Lepot et al. (2017).

intra-microfossil only localization of these Fe-minerals (Fig. 4d) contrasts strongly with post-mortem Fe-mineralization of walls by pyrite (Fig. 4a–c and Wacey et al., 2013) or siderite (Fig. 4a–c and Fadel et al., 2017). These Fe-minerals have been interpreted as the products of in-situ reductive recrystallization of intracellular Fe^{3+}-bearing biominerals. The combined C-isotopes signature (Williford et al., 2013), intracellular Fe-biomineralization, and microfossil morphology is best explained by cyanobacteria (Lepot et al., 2017). Evidence for chemotrophic Fe-oxidizing bacteria or photoferrotrophic bacteria are still lacking in stromatolitic Gunflint-type assemblages.

2.5. Chemotrophic Fe-oxidizing bacteria

Phosphatic stromatolites of the ~1.7 Ga Jhamarkotra Formation (Aravalli Group, India), display twisted Fe-oxide filaments similar to the Fe-biomineralized extracellular stalks of some chemolithoautotrophic bacteria (Crosby et al., 2014). Indeed, the freshwater iron-oxidizing bacteria *Gallionella ferruginea* and the marine *Mariprofundus ferrooxydans* both use O_2 (in microaerophilic conditions) to oxidize Fe^{2+}; both are able of chemolithoautotrophy, and *Gallionella* can also grow on organic compounds in addition to CO_2 (Emerson et al., 2010). They deposit Fe^{3+}-oxides onto twisted extracellular polysaccharide stalks that, together, withstand experimental diagenetic conditions (Picard et al., 2015).

2.6. Assemblages of deep-water cherts

Microfossil assemblages occur in chert nodules from the ~1.8 Ga Duck Creek Formation (Knoll et al., 1988; Schopf et al., 2015; Wilson et al., 2010) and the ~2.45–2.21 Ga Kazput Formation of the Turee Creek Group (Fadel et al., 2017; Schopf et al., 2015; Van Kranendonk et al., 2012), both from Western Australia. Their occurrence in massive dolomites and stratigraphic association suggest deposition in quiet, possibly relatively deep water (Barlow et al., 2016). Accordingly, unlike the stromatolitic Gunflint-type mats, these assemblages are not laminated but form cobweb-like structures. Some chert nodules of the Duck Creek Formation include the typical Gunflint-type assemblage with *Huroniospora*, *Eoastrion*, *Gunflintia,* and rare broad segmented filaments (Knoll et al., 1988). The cobweb-forming assemblages are, however, mostly composed of filamentous microorganisms. Some filaments ~ 8 μm in diameter displayed, under the optical microscope, microstructures suggesting elongated (12–15 μm) cells (Schopf et al., 2015). Dark, apparently unsegmented filaments ≤ 1 μm in diameter have been interpreted as filament-shaped single cells, unknown among cyanobacteria (Schopf et al., 2015); however, at the resolution limit of optical microscopy, these are difficult to distinguish from collapsed sheaths of trichome-forming microorganisms (e.g. the narrower sheaths in Fig. 3b). The preservation of elongated cells in broad filaments and the single-cell nature of the narrower filaments require confirmation with nanoscale analyses. These morphological features, combined with the presence of pyrite bearing the signature of bacterial sulfate-reduction have been used to propose that the cobweb-forming assemblages represent sulfur-cycling consortia (sulfuretum). Indeed, sulfate-reducing bacteria (Fukui et al., 1999), in addition to cyanobacteria (Wood et al., 2008), may form filaments with large, elongated shape. In the inferred sulfuretum, the broad (> 12 μm) filaments (Knoll et al., 1988) and the *Huroniospora* coccoids (Schopf et al., 2015) may represent sulfur-oxidizing bacteria such as *Beggiatoa/Thioploca* and *Thiovulum*, respectively, instead of cyanobacteria. In contrast, Wilson et al. (2010) proposed that the Duck Creek Formation assemblage was dominated by Fe-oxidizing bacteria. In a Turee Creek Group assemblage associated with a banded iron deposit, Fadel et al. (2017) observed a distinct cobweb-forming microfossil assemblage without segmented filaments or pyrite that would support SRB, and with siderite displaying isotopic signatures of Fe-deposition through oxidation, which is also consistent with chemotrophic or phototrophic (oxygenic or anoxygenic) Fe-oxidation.

2.7. Problematic fossil record

To our knowledge, the early Paleoproterozoic has a poor microfossil record. Rounded graphitic particles from the 2.5 Ga Hutuo Fm, China have been interpreted as possible highly metamorphosed acritarchs (Schiffbauer et al., 2007), but their biogenicity remains difficult to prove.

Other problematic traces consisting of U-shaped ridges in sandstone of the 2 to 1.8 Ga Stirling Range Formation, Australia, first reported as animal traces (Bengtson et al., 2007), have been reinterpreted as possible traces of giant protists such as amoebae, similar to observations in recent sediments (Bengtson and Rasmussen, 2009; Matz et al., 2008; Pawlowski and Gooday, 2009).

Recently discovered pyritic macrostructures from the 2.1 Ga Francevillian of Gabon have been interpreted as possible fossils of multicellular organisms, because of their large (~25 mm) size (El Albani et al., 2010). The term “multicellularity” implies only the occurrence of several cells, without evidence supporting either a prokaryotic or eukaryotic affinity (for reviews on multicellularity, see Butterfield, 2009; Knoll, 2011). These pyritic macrostructures only show traces of C and have been interpreted as organic masses pyritized by (likely heterotrophic) sulfate-reducing bacteria, as indicated by S-isotopes. So far they have been discriminated from abiotic pyrite concretions such as those described in Seilacher (2001) by details of their morphology showing soft deformation (folding), internal texture (mass of octahedral pyrite grains, different from the fibrous cone-in-cone texture of the “pyrite suns” of Seilacher, 2001), and distribution within the black shale beds draping them, deposited below an oxic water column in shallow water (Canfield et al., 2013; El Albani et al., 2010; El Albani et al., 2014) or under deeper water (> 200 m) (Parize et al., 2013). The identity of these macrostructures remains unknown and their biogenicity is questionable (e.g. Anderson et al., 2016) although the latter case study does not seem comparable.

2.8. Stromatolites

A general trend of increasing morphological diversity, size, and global distribution is observed in the stromatolitic record of carbonate rocks. From the Archean and early Proterozoic, through the mid-Proterozoic, stromatolite construction evolved from a texture mostly dominated by (bio)chemical carbonate precipitation with sparry microfabrics forming small (decimeter scale) cones and planar stromatolites (Allwood et al., 2009; Grotzinger and Knoll, 1999) to a more mixed and fine-grained texture of (bio)precipitation and trapping and binding of particles forming large domes (Buick, 1992; Coffey et al., 2013; Lepot et al., 2008; Lepot et al., 2009a), conic forms with a central column (Conophyton, e.g. Walter et al., 1976a), and digitate forms (Grey, 1994a, 1994b; Melezhik et al., 1997). Their biogenicity is most likely if stromatolites show complex morphologies, laterally and vertically variable laminae and organic bearing microfabrics, as these features are difficult to explain by abiotic mineral precipitation alone (see discussions of biogenicity criteria in Bosak et al., 2013; Grotzinger and Knoll, 1999). These changes might reflect changes in hydrodynamic and physico-chemical conditions, larger areas of shallow carbonate platforms, but also diversification of building microbial communities. Microstructural fabrics in Proterozoic stromatolites can sometimes provide a record of microbial community diversity despite diagenetic alteration (Knoll et al., 2013). Complex assemblages of stromatolites populate the 2.4–2.2 Ga Turee Creek group of Western Australia. Their complex morphologies (domical: e.g. Fig. 5a, columnar, thrombolitic, stratiform) may reflect changes in environments and microbial communities associated with the GOE (Barlow et al., 2016; Martindale et al., 2015). Two major events are noted in the Paleoproterozoic evolution of stromatolites on the Fennoscandian shield and include a maximum in diversity and abundance of stromatolites between 2330 and 2060 Ma ago, linked to cratonization, and a decline between 2060

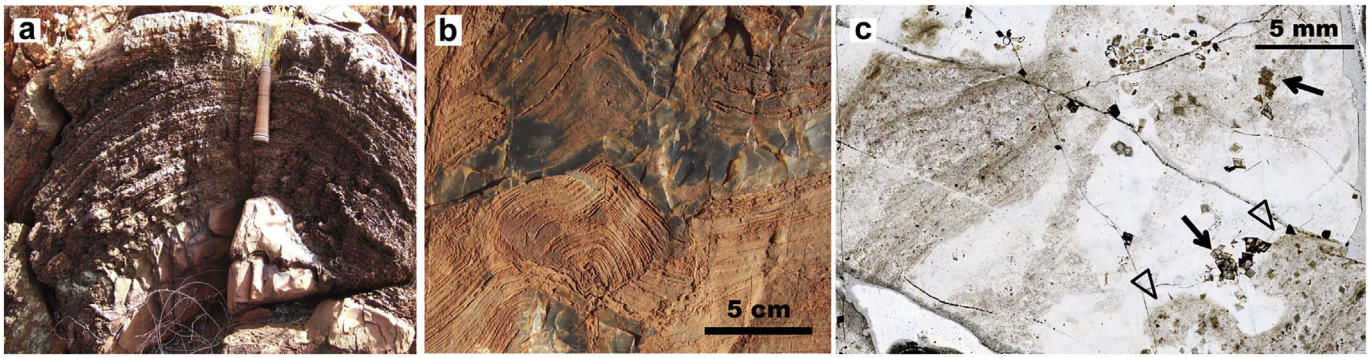

Fig. 5. Paleoproterozoic stromatolites. a. Outcrop picture of a meter-scale bulbous carbonate stromatolite from the Kazput Formation of the 2.45–2.21 Ga Turee Creek Group (see Barlow et al., 2016; Martindale et al., 2015 for details on the locality); hammer = 30 cm. b. Outcrop picture of a stromatolite from the ~1.8 Ga Duck Creek Formation (Wilson et al., 2010). Orange zones are mostly composed of carbonates. In black zones, carbonate laminae have been partly to completely replaced by chert. c. Thin section photomicrograph (5 × objective) of a stromatolite from the Gunflint Iron Formation at the Schrieber Beach locality. The stromatolites are essentially composed of quartz (white) with organic matter laminae (brown) forming bulges (arrowheads) or cones (top left corner). Carbonates are mainly present as dispersed, coarse ankerite [$(Fe,Ca,Mg)CO_3$] rhombohedra (arrows) of late diagenetic origin (Lepot et al., 2017).

and 1900 Ma ago, linked to oceanization and consequent decline of niches suitable for benthic cyanobacteria (Melezhik et al., 1997). Highly diverse and abundant stromatolites are also found in the late Paleoproterozoic of Western Australia (Grey, 1994a, 1994b). Paleogeographical differences in abundance and diversity patterns are reported between the Fennoscandia, India and China on one side, and Australia and northern America on the other side (Melezhik et al., 1997).

Late Paleoproterozoic stromatolites of the Aravalli Supergroup of India display abundant phosphatized granules intimately associated with organic matter, which have been proposed as possible phosphatized cells or phosphatized extracellular polymeric substances (Papineau et al., 2016). Stromatolites bearing Gunflint-type microfossil assemblages are siliceous and have been debated as resulting of primary silicification by hydrothermal fluids (Maliva et al., 2005) or as diagenetic cherts formed by replacement of primary carbonates (Petrash et al., 2016; Sommers et al., 2000). While the latter process is common in carbonate platform stromatolites (Fig. 5b), it remains difficult to distinguish from primary silica in stromatolites samples where carbonates are essentially represented by late-diagenetic rhombs (Fig. 5c). In our view, the question of the original mineralogy of many Paleoproterozoic siliceous stromatolites remains unanswered.

Microbially Induced Sedimentary Structures (MISS) preserved in siliciclastic deposits, are recorded from the Eoarchean to the present in intertidal environments (Noffke et al., 2013b), although the microorganisms responsible for their occurrence have changed from anaerobic to aerobic microorganisms (mostly cyanobacteria today). For a recent review of stromatolites and MISS, which is beyond the scope of this review, see Bosak et al. (2013) and Noffke et al. (2013a).

3. Implications for early biosphere evolution

The Paleoproterozoic microfossil assemblages include unambiguous eukaryotes difficult to relate to modern clades, cyanobacteria, iron-oxidizing and other undetermined filamentous and coccoidal prokaryotes, possible sulfur-oxidizing and/or sulfate-reducing bacteria, and heterotrophic decomposers (possibly including some sulfate-/iron-reducing bacteria, some mixotrophic sulfur-/iron-oxidizing bacteria, some methanogens and other fermenters) (Fig. 1). There are no unambiguous microfossils of the domain Archaea and their biomarker record (for the clade performing anaerobic oxidation of methane) is known from the Carboniferous (Birgel et al., 2008). The extremely light carbon-isotopic values at ~2.1 Ga (Weber and Gauthier-Lafaye, 2013) and between 2.8 and 2.6 Ga (or possibly as early as 3.5 Ga; Ueno et al., 2006) indicate the activities of methanogenic archaea and subsequent (archaeal and/or bacterial) methanotrophy (Eigenbrode et al., 2008; Hayes, 1994). However, Slotznick and Fischer (2016) suggested that methanotrophy was not responsible for the notably low $\delta^{13}C_{org}$ values (in the 2.72 Ga Tumbiana Formation, Australia), which may have formed through the reductive acetyl co-enzyme A (CoA) pathway. Because of the chimeric nature of the eukaryotic cell, which contains bacterial and archaeon genes, most models for the origin of eukaryotes involve the contribution of an archaea (see review in Lopez-Garcia and Moreira, 2015; Spang and Ettema, 2016), thus implying a preceding origin of the domain, although this is discussed (Eme and Doolittle, 2015; Gouy et al., 2015). Most major clades of the domain Bacteria had probably diversified already in the Paleoproterozoic, since cyanobacteria are not among the early diverging bacteria on phylogenetic reconstructions and had appeared at least by the time of the GOE, ~2.5 Ga ago (Pace, 1997; Schirrmeister et al., 2013).

This middle age biosphere diversified in a variety of new ecological niches. Mildly oxygenated shallow water of carbonate and siliciclastic platforms were colonized by cyanobacterial mats and stromatolites, probably other aerobe prokaryotes and by eukaryotes. Shallow-water stromatolites bearing Gunflint-type microfossil assemblages between 2.1 and 1.7 Ga display an enrichment in non-clastic, non-pyritic iron. This iron enrichment was likely associated with the transient return to ferruginous conditions associated with an increase of volcanic activity around 1.9–1.8 Ga (Rasmussen et al., 2012), and a post-GOE drop in oxygen as early as 2.1 Ga (Canfield et al., 2013; Lyons et al., 2014). Whether these assemblages developed in restricted or open-marine basins is unclear. In these conditions, oxygen produced by cyanobacteria may have been used by, and possibly nearly titrated, through iron oxidation and organic-matter respiration. Accordingly, observed intra-microfossil Fe-mineralization is consistent with Fe-tolerant cyanobacteria in the Gunflint Iron Formation (Lepot et al., 2017). The small amount of available sulfate was reduced by sulfate-reducing bacteria to sulfide (Wacey et al., 2013) that would have precipitated immediately with excess Fe^{2+}, hence limiting sulfur-oxidizing metabolism (such as anoxygenic photosynthesis) that is usually observed below cyanobacterial mats in modern stromatolites (Vasconcelos et al., 2006). Photoferrotrophs and Fe-oxidizing chemo(auto)trophs may also have contributed to the Gunflint-type assemblages, but morphological evidence of Fe-using chemoautotrophy appears only in 1.7 Ga stromatolites without other Gunflint-type microfossils (Crosby et al., 2014). Some non-stromatolitic, cobweb-forming microfossil assemblages from chert nodules in dolomites may have formed in distinct environmental conditions, possibly below the photic zone and/or within the sediment, where it could have derived energy from redox cycling of sulfur (Schopf et al., 2015) or iron (Fadel et al., 2017; Wilson et al., 2010). Although they share the assemblage of microfossils with simple morphological features (filaments, spheres and star shapes), Gunflint-type and

cobweb-forming assemblages may, in detail, be very heterogeneous in terms of microbial diversity and paleoenvironments. Additional morphometric studies resolved at the nanoscale, diversity assessment and abundance counting, coupled with geochemical characterization and sequence stratigraphy are required to better constrain the nature of these Paleoproterozoic ecosystems.

The Gunflint-type assemblages seem to have lasted from ~2.1 to 1.7 Ga and disappeared after the Paleoproterozoic (Sergeev, 2009). Oxygenic photosynthesis, possibly limited to Fe-tolerant cyanobacteria (Brown et al., 2010; Swanner et al., 2015) during the Paleoproterozoic, diversified after the subsequent withdrawal of ferruginous conditions to deeper water and through the proposed late Paleoproterozoic expansion of sulfidic subsurface waters (Shen et al., 2002) or spatially variable sulfidic wedges and restricted basins (Planavsky et al., 2011; Poulton et al., 2010). The latest Paleoproterozoic and younger strata (> 1.68 Ga) display an increased abundance of morphologically identified cyanobacteria (Knoll and Golubic, 1992; Schopf, 1992; Sharma, 2006a; Shi et al., 2017; Zhang and Golubic, 1987). Abundant putative akinete microfossils (Schopf, 1992; Sharma, 2006b) suggest that aerobic N_2-fixation was already performed as early as 1.6 Ga, and possibly as early as 2.1 Ga in some Gunflint-type assemblages (Amard and Bertrand Sarfati, 1997).

In the late Paleoproterozoic to early Neoproterozoic (1.8 to 0.8 Ga), the euxinic OMZ may have been colonized by microbes performing denitrification, anammox and anoxygenic photosynthesis (Johnston et al., 2009). Oceanic bottom waters stayed ferruginous and anoxic from the Neoarchean through the mid-to late Neoproterozoic, and were overlain by spatially variable euxinic water (layers or wedges), with brief returns to (possibly global) ferruginous conditions (e.g. at 1.9 Ga). These conditions, possibly limiting the availability of essential nutrients, may have restrained the diversification of life, especially the photosynthetic eukaryotes whose metallo-enzymes require more trace metals than the prokaryotic enzymes for N-fixation (Anbar and Knoll, 2002).

Several authors (Anbar and Knoll, 2002; Buick, 2007; Glass et al., 2009; Johnston et al., 2009; Konhauser et al., 2009) have proposed a link between changing ocean chemistry and the history of transition-metal availability through time, with possible profound implications on the evolution of marine primary producers. Indeed, these metals, such as Fe, Mo, Ni, Cu and V are used in prokaryotic and eukaryotic metalloenzymes to assimilate nitrogen. N is essential to all life, is abundant in the atmosphere in the form of N_2 gas, but only some bacteria (including some cyanobacterial taxa) and archaea are able to directly assimilate ("fix") N_2, whereas most taxa require "fixed" N in the form of ammonia, nitrates, nitrites, or amino acids. When oxygen started to accumulate, Mo would be mobilized and available for Mo-using enzymes. The subsequent euxinic conditions of the late Paleoproterozoic to early Neoproterozoic would have limited Mo and Fe availability (forming insoluble precipitates with sulfides) (Anbar and Knoll, 2002). These conditions would have discriminated against photosynthetic eukaryotes and in favor of cyanobacteria. Eukaryotes are indeed unable to fix N_2 and require higher levels of Mo to reduce nitrate and nitrite than cyanobacteria need to fix N_2 (Anbar and Knoll, 2002). However, Ni and Cu are also important metals used in N assimilation and the evolution of their availability through time is not known yet, although Ni might have been higher in the Archean Era (Konhauser et al., 2009), Cu and Cd lowest during the late Paleoproterozoic to early Neoproterozoic (Anbar and Knoll, 2002; Buick, 2007). Johnston et al. (2009) argued that fixed N would be scarce in these proterozoic oxygenated waters above the OMZ, because while ascending from deep waters, it would have been consumed by microbial denitrification, anammox (anaerobic ammonium oxidation) and anoxygenic photosynthesis in the OMZ. Therefore N-deficiency would have favored N_2-fixing bacteria over eukaryotic algae. In the OMZ, primary production would be dominated by anoxygenic photosynthesizers (including some cyanobacteria able to perform anoxygenic photosynthesis). Cyanobacteria and anoxygenic phototrophs may thus have dominated the primary production, consistent with the record of steroid biomarkers indicating that "bacteria were the only notable primary producers in the oceans before the Cryogenian period (720–635 Ma ago)" (Brocks et al., 2017).

The Paleoproterozoic cyanobacterial record is strongly biased toward shallow-water benthic assemblages, possibly due to the diagenetic environment favoring silicification. These assemblages may have embedded some planktonic cyanobacteria. However, the Paleoproterozoic cyanobacteria (chroococcales-, oscillatoriales- and nostocales-like) that could represent planktonic forms also commonly grow as benthos in modern environments (Golubic and Seong-Joo, 1999; Izaguirre et al., 2007; León-Tejera et al., 2011). Thus, the Paleoproterozoic record so far cannot confirm or invalidate i) hypotheses that cyanobacterial primary production and O_2 release were mostly from marine benthos or continental (freshwater and/or soil) origin (Lalonde and Konhauser, 2015) and ii) molecular clocks that suggest a late evolution of planktonic cyanobacteria (Sánchez-Baracaldo, 2015).

The complex (and still unresolved) Proterozoic history of changing ocean and atmosphere chemistry may have limited the diversification of eukaryotes outside of oxygenated nutrient-rich shallow waters, as suggested by paleoecological studies of microfossil assemblages from the ~1.5 Ga Roper Group (Javaux and Knoll, 2017; Javaux et al., 2001) and from the 1.1 Ga El Mreiti Group (Beghin et al., 2017), where the more diversified assemblages occur in marginal to shallow shelf facies, although one species of possible eukaryote also occurs in the Roper basinal anoxic facies. However, it is possible that heterotrophic protists feeding on particulate organic matter or bacteria, or anaerobic or dysaerobic protists may have been less affected than photosynthetic and aerobe eukaryotes. Detailed studies coupling microfossils, biomarkers and paleoecological analyses will permit to test this hypothesis. Indeed, some microfossils such as *Tappania plana* or *Trachyhystrichosphaera aimika* show a morphology suggesting osmotrophy (Beghin et al., 2017; Javaux and Knoll, 2017) and biomarker analyses in the late Mesoproterozoic show that crown-group algae were not detectable primary producers in the plankton (Brocks et al., 2017) even though benthic multicellular algae had appeared (Butterfield, 2000). The early diversity of eukaryotic microfossils, low in the Paleoproterozoic and moderate in the Mesoproterozoic (Javaux, 2011; Javaux and Knoll, 2017; Knoll et al., 2006), could result from the absence of preservable cell walls in many heterotrophs in comparison to algae, or the lack of diagnostic characters permitting their identification in the fossil record (Porter, 2006). Furthermore, there might also be a bias in the sampling record and in the preservation windows of the geological record (Cohen and Macdonald, 2015). It is also possible that simple morphologies (phenotypes) hide higher genetic diversity (genotypes) within microfossil assemblages.

The eukaryotic cell, with its flexible membrane, cytoskeleton and nucleus, appeared early, possibly in the late Archean but indisputably in the late Paleoproterozoic. The pattern of eukaryotic evolution may be divided into three periods differing by their level of diversification (Javaux, 2011). Period I, from at least 1.7 to ~1.1 Ga, was a time of moderate stem group diversification (not excluding the possibility of crown groups), followed by a major diversification at the level of supergroups in the late Mesoproterozoic-early Neoproterozoic (Period II, ~1.1 to 0.635 Ga). Period I records the evolution of major biological innovations, such as a flexible membrane, a cytoskeleton, a nucleus, multicellularity, different life stages and excystment structures, osmotrophy and heterotrophy, reproduction by budding and binary division, probably meiosis (sex), benthic life style and macroscopic size (Javaux, 2007; Javaux and Knoll, 2017). During Period II, cellular differentiation, protist biomineralization, protist predation, and eukaryotic photosynthesis had evolved (the latter possibly earlier but this remains to be confirmed). The Ediacarian Period (Period III) was marked by a greater morphological diversification but within the pre-existing supergroups, including the diversification of early animals, adding a new level of predation pressure. This pattern of eukaryotic evolution may

possibly be related to environmental conditions (e.g. Guilbaud et al., 2015), but also ecological complexification and biological innovations, such as the acquisition of the chloroplast, the rise of protist predation (Knoll, 2014; Knoll and Lahr, 2016; Porter, 2011; Porter, 2016) and animal predation (Butterfield, 2015a), and possibly of toxic protists (Brocks et al., 2016). Period II coincides with changing conditions in the atmosphere and oceans, the supercontinent Rodinia amalgamation and break-up, and major glaciations. Thus, the limitation of trace-element availability might not explain completely the observed pattern after all, since the diversification of eukaryotes (whether they represent modern supergroups or stem groups), started during the "boring billion" (1.8 to 0.8 Ga) (Javaux, 2011; Javaux et al., 2013) and before the demise of stratified ocean conditions around 0.58 Ga (Canfield et al., 2008).

The Paleoproterozoic began with major environmental changes, including oxygenation of the atmosphere and oceans, the supercontinent Kenorland break-up (Reddy and Evans, 2009), and major glaciations, and was a time of biological diversification (Fig. 1). New organisms appeared: various cyanobacteria, followed by deep-water cobweb-forming communities that likely mediated S/Fe oxidation, followed by Gunflint-type shallow-water benthic assemblages that likely hosted photosynthetic biomass, and then, eukaryotes. Most of the Gunflint-type assemblages disappeared after the Paleoproterozoic, although ferruginous conditions persisted later but dominantly in deep bottom water. Iron-oxidizing bacteria persist today in iron-rich environments (Konhauser, 2007) but their similarity to Gunflint assemblages is unknown. Cyanobacteria and eukaryotes continued to diversify in increasingly oxygenated niches. Phylogenetic and ultrastructural studies show that the common ancestor of extant eukaryotes (but not necessarily the first eukaryote) was a protist with mitochondria (Cavalier-Smith, 2009; Embley and Martin, 2006). This may suggest that the diversification of modern eukaryotes could have started once the oxygen-producing cyanobacteria and the proteobacterial ancestor of the mitochondria had appeared (Javaux, 2011). However, recent studies show that mitochondria can be facultatively anaerobic (Mentel and Martin, 2008), but the ancestral or secondary state of this capability is so far unknown. Another study showed that eukaryotic sterol synthesis could be performed by yeast at very low oxygen concentration, similar to pre-GOE conditions, suggesting that the presence of sterols cannot be used to infer past atmospheric oxygen levels as previously assumed (Waldbauer et al., 2011). However, this may again result from secondary adaptation as well as from an ancestral ability. Modern anaerobe eukaryotes evolved from secondary adaptation, but perhaps early eukaryotes were anaerobic or dysaerobic, and did not require an oxygenated world to appear and diversify early. However, Gold et al. (2017) recently suggested that bacterial and eukaryotic sterol synthesis diverged around 2.31 Ga, at the time of the GOE. Detailed coupled studies of microfossil assemblages and redox conditions may help to resolve this issue (e.g. Beghin et al., 2017; Guilbaud et al., 2015; Javaux et al., 2013; Johnston et al., 2010).

4. Conclusions

Collectively, the unambiguous Paleoproterozoic microfossil record illustrates biosphere evolution during a time of chemical changes in the oceans and the atmosphere. The fossil assemblages include iron-loving and other undetermined filamentous and coccoidal prokaryotes, eukaryotes, and modern cyanobacteria taxa. Early eukaryotic crown-group diversification may have been restrained in the Paleoproterozoic by ocean-chemistry conditions, but it increased during the late Mesoproterozoic–early Neoproterozoic despite the continuation of similar conditions, then amplified significantly (but perhaps within lower taxonomic levels), with the demise of euxinic conditions and increase in ecological complexity. The so-called "boring billion" is thus mis-called, as it was actually a fascinating time of life diversification, including complex life.

The emerging picture is one of a changing and more complex biosphere in which the three domains of life, Archaea, Bacteria and Eukarya, were diversifying in various ecological niches marked by the diversification of identified microfossils, stromatolites, increasing abundance of preserved biomarkers and appearance of macroscopic problematic fossils or trace fossils.

Acknowledgments

We would like to thank the issue editors Simon Poulton and David Johnston for their invitation to write this paper. We are also grateful to Andy H. Knoll for providing some of the pictures. Some of the illustrated microfossils have been studied from rock samples provided by S. Xiao, M. Walter, A.H. Knoll, P. Medvedev, and the FAR-DEEP project, who are also thanked. Comments by Susannah Porter, three anonymous reviewers, and the Editor (André Strasser) are much appreciated and helped to improve the manuscript.

Funding: This work was supported by the EU FP7-ERC StG ELiTE [grant number 308074]; the Belspo IAP PLANET TOPERS; the Francqui Foundation; the FNRS [grant number FRFC 2.4.558.09.F]; the Région Hauts-de-France project Visionn'AIRR [grant number iM4] and the ANR M6fossils [grant number ANR-15-CE31-0003-01].

References

Adam, Z.R., Skidmore, M.L., Mogk, D.W., Butterfield, N.J., 2017. A Laurentian record of the earliest fossil eukaryotes. Geology 45, 387–390.
Agić, H., Moczydłowska, M., Yin, L.-M., 2015. Affinity, life cycle, and intracellular complexity of organic-walled microfossils from the Mesoproterozoic of Shanxi. China. J. Paleontol. 89, 28–50.
Alleon, J., Bernard, S., Le Guillou, C., Daval, D., Skouri-Panet, F., Pont, S., Delbes, L., Robert, F., 2016a. Early entombment within silica minimizes the molecular degradation of microorganisms during advanced diagenesis. Chem. Geol. 437, 98–108.
Alleon, J., Bernard, S., Le Guillou, C., Marin-Carbonne, J., Pont, S., Beyssac, O., McKeegan, K.D., Robert, F., 2016b. Molecular preservation of 1.88 Ga Gunflint organic microfossils as a function of temperature and mineralogy. Nat. Commun. 7, 11977.
Allwood, A.C., Grotzinger, J.P., Knoll, A.H., Burch, I.W., Anderson, M.S., Coleman, M.L., Kanik, I., 2009. Controls on development and diversity of early Archean stromatolites. Proc. Natl. Acad. Sci. U. S. A. 106, 9548–9555.
Amard, B., Bertrand Sarfati, J., 1997. Microfossils in 2000 Ma old cherty stromatolites of the Franceville group, Gabon. Precambrian Res. 81, 197–221.
Anbar, A.D., Knoll, A.H., 2002. Proterozoic ocean chemistry and evolution: a bioinorganic bridge? Science 297.
Anbar, A.D., Duan, Y., Lyons, T.W., Arnold, G.L., Kendall, B., Creaser, R.A., Kaufman, A.J., Gordon, G.W., Scott, C., Garvin, J., Buick, R., 2007. A whiff of oxygen before the great oxidation event. Science 317, 1903.
Anderson, R.P., Tarhan, L.G., Cummings, K.E., Planavsky, N.J., Bjornerud, M., 2016. Macroscopic structures in the 1.1 Ga continental Copper Harbor formation: concretions or fossils? PALAIOS 31, 327–338.
Arouri, K., Greenwood, P.F., Walter, M.R., 1999. A possible chlorophycean affinity of some Neoproterozoic acritarchs. Org. Geochem. 30, 1323–1337.
Arouri, K., Greenwood, P.F., Walter, M.R., 2000. Biological affinities of Neoproterozoic acritarchs from Australia: microscopic and chemical characterisation. Org. Geochem. 31, 75–89.
Awramik, S.M., Barghoorn, E.S., 1977. The Gunflint microbiota. Precambrian Res. 5, 121–142.
Barghoorn, E.S., Tyler, S.A., 1965. Microorganisms from the Gunflint Chert. Science 147, 563–575.
Barley, M.E., Bekker, A., Krapez, B., 2005. Late Archean to Early Paleoproterozoic global tectonics, environmental change and the rise of atmospheric oxygen. Earth Planet. Sci. Lett. 238, 156–171.
Barlow, E., Van Kranendonk, M.J., Yamaguchi, K.E., Ikehara, M., Lepland, A., 2016. Lithostratigraphic analysis of a new stromatolite-thrombolite reef from across the rise of atmospheric oxygen in the Paleoproterozoic Turee Creek group, Western Australia. Geobiology 14, 317–343.
Beghin, J., Storme, J.Y., Blanpied, C., Gueneli, N., Brocks, J.J., Poulton, S.W., Javaux, E.J., 2017. Microfossils from the late Mesoproterozoic–early Neoproterozoic Atar/El Mreïti Group, Taoudeni Basin, Mauritania, northwestern Africa. Precambrian Res. 291, 63–82.
Bekker, A., Holland, H.D., 2012. Oxygen overshoot and recovery during the early Paleoproterozoic. Earth Planet. Sci. Lett. 317-318, 295–304.
Bekker, A., Holland, H.D., Wang III, P.-L., Dr Stein, H.J., Hannah, J.L., Coetzee, L.L., Beukes, N.J., 2004. Dating the rise of atmospheric oxygen. Nature 427, 117–120.
Bengtson, S., Rasmussen, B., 2009. PALEONTOLOGY new and ancient trace makers. Science 323, 346–347.
Bengtson, S., Rasmussen, B., Krapez, B., 2007. The Paleoproterozoic megascopic Stirling biota. Paleobiology 33, 351–381.

Bengtson, S., Belivanova, V., Rasmussen, B., Whitehouse, M., 2009. The controversial "Cambrian" fossils of the Vindhyan are real but more than a billion years older. Proc. Natl. Acad. Sci. U. S. A. 106, 7729–7734.
Bengtson, S., Sallstedt, T., Belivanova, V., Whitehouse, M., 2017. Three-dimensional preservation of cellular and subcellular structures suggests 1.6 billion-year-old crown-group red algae. PLoS Biol. 15, e2000735.
Bernard, S., Benzerara, K., Beyssac, O., Menguy, N., Guyot, F., Brown, G.E., Goffe, B., 2007. Exceptional preservation of fossil plant spores in high-pressure metamorphic rocks. Earth Planet. Sci. Lett. 262, 257–272.
Birgel, D., Himmler, T., Freiwald, A., Peckmann, J., 2008. A new constraint on the antiquity of anaerobic oxidation of methane: Late Pennsylvanian seep limestones from southern Namibia. Geology 36, 543–546.
Boal, D., Ng, R., 2010. Shape analysis of filamentous Precambrian microfossils and modern cyanobacteria. Paleobiology 36, 555–572.
Bosak, T., Knoll, A.H., Petroff, A.P., 2013. The meaning of stromatolites. Annu. Rev. Earth Planet. Sci. 41, 21–44.
Brasier, M.D., Green, O.R., Lindsay, J.F., McLoughlin, N., Steele, A., Stoakes, C., 2005. Critical testing of earth's oldest putative fossil assemblage from the similar to 3.5 Ga Apex Chert, Chinaman Creek, western Australia. Precambrian Res. 140, 55–102.
Brasier, M.D., Antcliffe, J., Saunders, M., Wacey, D., 2015. Changing the picture of Earth's earliest fossils (3.5–1.9 Ga) with new approaches and new discoveries. Proc. Natl. Acad. Sci. U. S. A. 112, 4859–4864.
Brocks, J.J., Buick, R., Summons, R.E., Logan, G.A., 2003. A reconstruction of Archean biological diversity based on molecular fossils from the 2.78 to 2.45 billion-year-old Mount Bruce Supergroup, Hamersley Basin, Western Australia. Geochim. Cosmochim. Acta 67, 4321–4335.
Brocks, J.J., Love, G.D., Summons, R.E., Knoll, A.H., Logan, G.A., Bowden, S.A., 2005. Biomarker evidence for green and purple sulphur bacteria in a stratified Palaeoproterozoic sea. Nature 437, 866–870.
Brocks, J.J., Grosjean, E., Logan, G.A., 2008. Assessing biomarker syngeneity using branched alkanes with quaternary carbon (BAQCs) and other plastic contaminants. Geochim. Cosmochim. Acta 72, 871–888.
Brocks, J.J., Jarrett, A.J.M., Sirantoine, E., Kenig, F., Moczydlowska, M., Porter, S., Hope, J., 2016. Early sponges and toxic protists: possible sources of cryostane, an age diagnostic biomarker antedating Sturtian snowball earth. Geobiology 14, 129–149.
Brocks, J.J., Jarrett, A.J.M., Sirantoine, E., Hallmann, C., Hoshino, Y., Liyanage, T., 2017. The rise of algae in Cryogenian oceans and the emergence of animals. Nature 548, 578–581.
Brown, I.I., Bryant, D.A., Casamatta, D., Thomas-Keprta, K.L., Sarkisova, S.A., Shen, G., Graham, J.E., Boyd, E.S., Peters, J.W., Garrison, D.H., McKay, D.S., 2010. Polyphasic characterization of a thermotolerant siderophilic filamentous cyanobacterium that produces intracellular iron deposits. Appl. Environ. Microbiol. 76, 6664–6672.
Buick, R., 1990. Microfossil recognition in Archean rocks; an appraisal of spheroids and filaments from a 3500 m.y. old chert-barite unit at North Pole, Western Australia. PALAIOS 5, 441–459.
Buick, R., 1992. The antiquity of oxygenic photosynthesis - evidence from stromatolites in sulfate-deficient Archean lakes. Science 255, 74–77.
Buick, R., 2007. Did the Proterozoic 'Canfield Ocean' cause a laughing gas greenhouse? Geobiology 5, 97–100.
Buick, R., 2008. When did oxygenic photosynthesis evolve? Philos. Trans. R. Soc. B-Biol. Sci. 363, 2731–2743.
Butterfield, N.J., 2000. *Bangiomorpha pubescens* n. gen., n. sp.: implications for the evolution of sex, multicellularity, and the Mesoproterozoic/Neoproterozoic radiation of eukaryotes. Paleobiology 26, 386–404.
Butterfield, N.J., 2009. Modes of pre-Ediacaran multicellularity. Precambrian Res. 173, 201–211.
Butterfield, N.J., 2015a. Early evolution of the Eukaryota. Palaeontology 58, 5–17.
Butterfield, N.J., 2015b. Proterozoic photosynthesis - a critical review. Palaeontology 58, 953–972.
Canfield, D.E., 1998. A new model for Proterozoic ocean chemistry. Nature 396, 450–453.
Canfield, D.E., Poulton, S.W., Knoll, A.H., Narbonne, G.M., Ross, G., Goldberg, T., Strauss, H., 2008. Ferruginous conditions dominated later neoproterozoic deep-water chemistry. Science 321, 949–952.
Canfield, D.E., Ngombi-Pemba, L., Hammarlund, E.U., Bengtson, S., Chaussidon, Marc, Gauthier-Lafaye, F., Meunier, A., Riboulleau, A., Rollion-Bard, C., Rouxel, O., Asael, D., Pierson-Wickmann, A.-C., Albani, A.E., 2013. Oxygen dynamics in the aftermath of the great oxidation of Earth's atmosphere. Proc. Natl. Acad. Sci. U. S. A. 110, 16736–16741.
Cavalier-Smith, T., 2009. Megaphylogeny, cell body plans, adaptive zones: causes and timing of eukaryote basal radiations. J. Eukaryot. Microbiol. 56, 26–33.
Chakrabarti, G., Shome, D., Kumar, S., Stephens, G.M., Kah, L.C., 2014. Carbonate platform development in a Paleoproterozoic extensional basin, Vempalle formation, Cuddapah Basin, India. J. Asian Earth Sci. 91, 263–279.
Chalansonnet, S., Largeau, C., Casadevall, E., Berkaloff, C., Peniguel, G., Couderc, R., 1988. Cyanobacterial resistant biopolymers. Geochemical implications of the properties of Schizotrix sp. resistant material. Org. Geochem. 13, 1003–1010.
Cloud, P., 1965. Significance of the gunflint (Precambrian) microflora. Science 148, 27–35.
Cloud, P.E., Hagen, H., 1965. Electron microscopy of the Gunflint microflora: preliminary results. Proc. Natl. Acad. Sci. U. S. A. 54, 1–8.
Cloud, P., Morrison, K., 1980. New microbial fossils from 2-gyr old rocks in northern Michigan. Geomicrobiol J. 2, 161–178.
Coffey, J.M., Flannery, D.T., Walter, M.R., George, S.C., 2013. Sedimentology, stratigraphy and geochemistry of a stromatolite biofacies in the 2.72 Ga Tumbiana Formation, Fortescue Group, Western Australia. Precambrian Res. 236, 282–296.
Cohen, P.A., Macdonald, F.A., 2015. The Proterozoic record of eukaryotes. Paleobiology 41, 610–632.
Cohen, P.A., Knoll, A.H., Kodner, R.B., 2009. Large spinose microfossils in Ediacaran rocks as resting stages of early animals. Proc. Natl. Acad. Sci. U. S. A. 106, 6519–6524.
Condie, K.C., O'Neill, C., Aster, R.C., 2009. Evidence and implications for a widespread magmatic shutdown for 250 my on earth. Earth Planet. Sci. Lett. 282, 294–298.
Cosmidis, J., Templeton, A.S., 2016. Self-assembly of biomorphic carbon/sulfur microstructures in sulfidic environments. Nat. Commun. 7, 12812.
Cosmidis, J., Benzerara, K., Menguy, N., Arning, E., 2013. Microscopy evidence of bacterial microfossils in phosphorite crusts of the Peruvian shelf: implications for phosphogenesis mechanisms. Chem. Geol. 359, 10–22.
Crosby, C.H., Bailey, J.V., Sharma, M., 2014. Fossil evidence of iron-oxidizing chemolithotrophy linked to phosphogenesis in the wake of the great oxidation event. Geology 42, 1015–1018.
Crowe, S.A., Dossing, L.N., Beukes, N.J., Bau, M., Kruger, S.J., Frei, R., Canfield, D.E., 2013. Atmospheric oxygenation three billion years ago. Nature 501, 535.
de Leeuw, J.W., Versteegh, G.J.M., van Bergen, P.F., 2006. Biomacromolecules of algae and plants and their fossil analogues. Plant Ecol. 182, 209–233.
Edwards, C.T., Pufahl, P.K., Hiatt, E.E., Kyser, T.K., 2012. Paleoenvironmental and taphonomic controls on the occurrence of Paleoproterozoic microbial communities in the 1.88 Ga Ferriman Group, Labrador Trough, Canada. Precambrian Res. 212, 91–106.
Eigenbrode, J.L., Freeman, K.H., Summons, R.E., 2008. Methylopane biomarker hydrocarbons in Hamersley Province sediments provide evidence for Neoarchean aerobiosis. Earth Planet. Sci. Lett. 273, 323–331.
El Albani, A., Bengtson, S., Canfield, D.E., Bekker, A., Macchiarelli, R., Mazurier, A., Hammarlund, E.U., Boulvais, P., Dupuy, J.-J., Fontaine, Claude, Fürsich, F.T., Gauthier-Lafaye, F., Janvier, P., Javaux, E., Ossa, F.O., Pierson-Wickmann, A.-C., Riboulleau, A., Sardini, P., Vachard, D., Whitehouse, M., Meunier, A., 2010. Large colonial organisms with coordinated growth in oxygenated environments 2.1 Gyr ago. Nature 466, 100–104.
El Albani, A., Bengtson, S., Canfield, D.E., Riboulleau, A., Rollion-Bard, C., Macchiarelli, R., Ngombi Pemba, L., Hammarlund, E., Meunier, Alain, Moubiya Mouele, I., Benzerara, K., Bernard, S., Boulvais, P., Chaussidon, M., Cesari, C., Fontaine, C., Chi-Fru, E., Garcia Ruiz, J.M., Gauthier-Lafaye, F., Mazurier, A., Pierson-Wickmann, A.C., Rouxel, O., Trentesaux, A., Vecoli, M., Versteegh, G.J.M., White, L., Whitehouse, M., Bekker, A., 2014. The 2.1 Ga old Francevillian biota: biogenicity, taphonomy and biodiversity. PLoS One e99438, 9.
Embley, T.M., Martin, W., 2006. Eukaryotic evolution, changes and challenges. Nature 440, 623–630.
Eme, L., Doolittle, W.F., 2015. Archaea. Curr. Biol. 25, 851–855.
Eme, L., Sharpe, S.C., Brown, M.W., Roger, A.J., 2014. On the age of eukaryotes: evaluating evidence from fossils and molecular clocks. Cold Spring Harb. Perspect. Biol. 6, a016139.
Emerson, D., Fleming, E.J., McBeth, J.M., 2010. Iron-oxidizing bacteria: an environmental and genomic perspective. Annu. Rev. Microbiol. 64, 561–583.
Fadel, A., Lepot, K., Busigny, V., Addad, A., Troadec, D., 2017. Iron mineralization and taphonomy of microfossils of the 2.45–2.21 Ga Turee Creek group, Western Australia. Precambrian Res. 298, 530–551.
Fischer, W.W., Hemp, J., Johnson, J.E., 2016. Evolution of oxygenic photosynthesis. Annu. Rev. Earth Planet. Sci. 44, 647–683.
Flannery, E.N., George, S.C., 2014. Assessing the syngeneity and indigeneity of hydrocarbons in the ~1.4 Ga Velkerri formation, McArthur Basin, using slice experiments. Org. Geochem. 77, 115–125.
Foucher, F., Ammar, M.-R., Westall, F., 2015. Revealing the biotic origin of silicified Precambrian carbonaceous microstructures using Raman spectroscopic mapping, a potential method for the detection of microfossils on Mars. J. Raman Spectrosc. 46, 873–879.
Fralick, P., Davis, D.W., Kissin, S.A., 2002. The age of the Gunflint Formation, Ontario, Canada: single zircon U-Pb age determinations from reworked volcanic ash. Can. J. Earth Sci. 39, 1085–1091.
Frei, R., Gaucher, C., Poulton, S.W., Canfield, D.E., 2009. Fluctuations in Precambrian atmospheric oxygenation recorded by chromium isotopes. Nature 461, 250–253.
French, K.L., Hallmann, C., Hope, J.M., Schoon, P.L., Zumberge, J.A., Hoshino, Y., Peters, C.A., George, S.C., Love, G.D., Brocks, J.J., Buick, R., Summons, R.E., 2015. Reappraisal of hydrocarbon biomarkers in Archean rocks. Proc. Natl. Acad. Sci. U. S. A. 112, 5915–5920.
Fukui, M., Teske, A., Aßmus, B., Muyzer, G., Widdel, F., 1999. Physiology, phylogenetic relationships, and ecology of filamentous sulfate-reducing bacteria (genus *Desulfonema*). Arch. Microbiol. 172, 193–203.
García Ruiz, J.M., Carnerup, A., Christy, A.G., Welham, N.J., Hyde, S.T., 2002. Morphology: an ambiguous indicator of biogenicity. Astrobiology 2, 353–369.
Garvin, J., Buick, R., Anbar, A.D., Arnold, G.L., Kaufman, A.J., 2009. Isotopic evidence for an aerobic nitrogen cycle in the latest Archean. Science 323, 1045–1048.
Glass, J.B., Wolfe-Simon, F., Anbar, A.D., 2009. Coevolution of metal availability and nitrogen assimilation in cyanobacteria and algae. Geobiology 7, 100–123.
Gold, D.A., Caron, A., Fournier, G.P., Summons, R.E., 2017. Paleoproterozoic sterol biosynthesis and the rise of oxygen. Nature 543, 420–423.
Golubic, S., Hofmann, H.J., 1976. Comparison of Holocene and mid-Precambrian entophysalidaceae (cyanophyta) in stromatolitic algal mats - cell-division and degradation. J. Paleontol. 50, 1074–1082.
Golubic, S., Seong-Joo, L., 1999. Early cyanobacterial fossil record: preservation, palaeoenvironments and identification. Eur. J. Phycol. 34, 339–348.
Gouy, R., Baurain, D., Philippe, H., 2015. Rooting the tree of life: the phylogenetic jury is still out. Philos. Trans. R. Soc. B-Biol. Sci. 370, 20140329.
Grey, K., 1994a. Stromatolites from the Palaeoproterozoic (Orosirian) Glengarry group,

Glengarry Basin, Western Australia. Alcheringa 18, 275–300.
Grey, K., 1994b. Stromatolites from the Palaeoproterozoic Earaheedy group, Earaheedy Basin, Western Australia. Alcheringa 18, 187–218.
Grotzinger, J.P., Knoll, A.H., 1999. Stromatolites in precambrian carbonates: evolutionary mileposts or environmental dipsticks? Annu. Rev. Earth Planet. Sci. 27, 313–358.
Guilbaud, R., Poulton, S.W., Butterfield, N.J., Zhu, M., Shields-Zhou, G.A., 2015. Global transition to ferruginous conditions in the early Neoproterozoic oceans. Nature. Geosciences 8, 466–470.
Han, T.M., Runnegar, B., 1992. Megascopic eukaryotic algae from the 2.1 billion-year-old Negaunee iron-formation. Science 257, 232–235.
Hannah, J.L., Bekker, A., Stein, H.J., Markey, R.J., Holland, H.D., 2004. Primitive Os and 2316 Ma age for marine shale: implications for Paleoproterozoic glacial events and the rise of atmospheric oxygen. Earth Planet. Sci. Lett. 225, 43–52.
Hayes, J.M., 1994. Global methanotrophy at the Archean-Proterozoic transition. In: Bengtson, S. (Ed.), Early Life on Earth. Nobel Symp. Columbia University Press, New York, pp. 220–236.
Hofmann, H.J., 1976. Precambrian microfolora, Belcher Islands, Canada: significance and systematics. J. Paleontol. 50, 1040–1073.
Hofmann, H.J., 1999. Global distribution of the Proterozoic sphaeromorph acritarch Valeria Lophostriata (Jankauskas). Acta Micropalaeo. Sin. 16, 215–224.
Hofmann, H.J., Schopf, J.W., 1983. Early Proterozoic microfossils. In: Schopf, J.W. (Ed.), Earth's Earliest Biosphere: Its Origin and Evolution. Princeton Univ. Press, Princeton, NJ, pp. 321–360.
House, C.H., Schopf, J.W., McKeegan, K.D., Coath, C.D., Harrison, T.M., Stetter, K.O., 2000. Carbon isotopic composition of individual Precambrian microfossils. Geology 28, 707–710.
Hu, G., Zhao, T., Zhou, Y., 2014. Depositional age, provenance and tectonic setting of the Proterozoic Ruyang group, southern margin of the North China craton. Precambrian Res. 246, 296–318.
Izaguirre, G., Jungblut, A.-D., Neilan, B.A., 2007. Benthic cyanobacteria (Oscillatoriaceae) that produce microcystin-LR, isolated from four reservoirs in southern California. Water Res. 41, 492–498.
Javaux, E.J., 2007. The early eukaryotic fossil record. In: Jekely, G. (Ed.), Origins and Evolution of Eukaryotic Endomembranes and Cytoskeleton. Landes Biosciences, TX, USA, pp. 1–19.
Javaux, E.J., 2011. Evolution of early eukaryotes in Precambrian oceans. In: Gargaud, M., López-García, P., Martin, H. (Eds.), Origins and Evolution of Life: An Astrobiological Perspective. Cambridge University Press, Cambridge, pp. 414–449.
Javaux, E.J., Benzerara, K., 2009. Microfossils. C. R. Palevol 8, 605–615.
Javaux, E.J., Knoll, A.H., 2017. Micropaleontology of the lower Mesoproterozoic Roper Group, Australia, and implications for early eukaryotic evolution. J. Paleontol. 91, 199–229.
Javaux, E.J., Marshall, C.P., 2006. A new approach in deciphering early protist paleobiology and evolution: combined microscopy and microchemistry of single Proterozoic acritarchs. Rev. Palaeobot. Palynol. 139, 1–15.
Javaux, E.J., Knoll, A.H., Walter, M.R., 2001. Morphological and ecological complexity in early eukaryotic ecosystems. Nature 412, 66–69.
Javaux, E.J., Knoll, A.H., Walter, M., 2003. Recognizing and interpreting the fossils of early eukaryotes. Orig. Life Evol. Biosph. 33, 75–94.
Javaux, E.J., Knoll, A.H., Walter, M.R., 2004. TEM evidence for eukaryotic diversity in mid-Proterozoic oceans. Geobiology 2, 121–132.
Javaux, E.J., Marshal, C.P., Bekker, A., 2010. Organic-walled microfossils in 3.2-billion-year-old shallow-marine siliciclastic deposits. Nature 463, 934–938.
Javaux, E.J., Lepot, K., van Zuilen, M., Melezhik, V.A., Medvedev, P.V., 2012. Palaeoproterozoic microfossils. In: Melezhik, V., Prave, A.R., Hanski, E.J., Fallick, A.E., Lepland, A., Kump, L.R., Strauss, H. (Eds.), Reading the Archive of Earth's Oxygenation. Springer, pp. 1352–1371.
Javaux, E.J., Beghin, J., Houzay, J.-P., Blanpied, C., 2013. The “boring billion”: an exciting time for early eukaryotes. Mineral. Mag. 77, 1380.
Johnston, D.T., Wolfe-Simon, F., Pearson, A., Knoll, A.H., 2009. Anoxygenic photosynthesis modulated Proterozoic oxygen and sustained Earth's middle age. Proc. Natl. Acad. Sci. U. S. A. 106, 16925–16929.
Johnston, D.T., Poulton, S.W., Dehler, C., Porter, S., Husson, J., Canfield, D.E., Knoll, A.H., 2010. An emerging picture of Neoproterozoic ocean chemistry: insights from the Chuar Group, Grand Canyon, USA. Earth Planet. Sci. Lett. 290, 64–73.
Kaźmierczak, J., 1979. The eukaryotic nature of Eosphaera-like ferriferous structures from the Precambrian Gunflint iron formation, Canada: a comparative study. Precambrian Res. 9, 1–22.
Kaźmierczak, J., Kremer, B., Altermann, W., Franchi, I., 2016. Tubular microfossils from ~2.8 to 2.7 Ga-old lacustrine deposits of South Africa: a sign for early origin of eukaryotes? Precambrian Res. 286, 180–194.
Kempe, A., Wirth, R., Altermann, W., Stark, R.W.S., William, J., Heckl, W.M., 2005. Focussed ion beam preparation and in situ nanoscopic study of Precambrian acritarchs. Precambrian Res. 140, 36–54.
Klein, C., Beukes, N.J., Schopf, J.W., 1987. Filamentous microfossils in the early Proterozoic Transvaal Supergroup: their morphology, significance and paleoenvironmental setting. Precambrian Res. 36, 81–94.
Kleinteich, J., Golubic, S., Pessi, I.S., Velázquez, D., Storme, J.Y., Darchambeau, F., Javaux, E.J., 2017. Cyanobacterial contribution to travertine deposition in the Hoyoux River system, Belgium. Microb. Ecol. 1–21.
Knoll, A.H., 2003. Life on a Young Planet, the First three billion Years of Evolution on Earth. Princeton University Press, Princeton.
Knoll, A.H., 2011. The multiple origins of complex multicellularity. Annu. Rev. Earth Planet. Sci. 39, 217–239.
Knoll, A.H., 2014. Paleobiological perspectives on early eukaryotic evolution. Cold Spring Harb. Perspect. Biol. 6, a016121.
Knoll, A.H., Golubic, S., 1992. Proterozoic and living cyanobacteria. In: Schidlowski, M., Golubic, S., Kimberley, M.M. (Eds.), Early Organic Evolution: Implications for Mineral and Energy Resources. Springer, Berlin-Heidelberg, pp. 450–462.
Knoll, A.H., Lahr, D.J., 2016. Fossils, feeding, and the evolution of complex multicellularity. In: Niklas, K.J., Newman, S.A. (Eds.), Multicellularity: Origins and Evolution. Vienna Series in Theoretical Biology. The MIT Press, pp. 3–16.
Knoll, A.H., Simonson, B., 1981. Early Proterozoic microfossils and penecontemporaneous quartz cementation in the Sokoman Iron Formation, Canada. Science 211, 478–480.
Knoll, A.H., Barghoorn, E.S., Awramik, S.M., 1978. New microorganisms from the Aphebian Gunflint iron formation, Ontario. J. Paleontol. 52, 976–992.
Knoll, A.H., Strother, P.K., Rossi, S., 1988. Distribution and diagenesis of microfossils from the lower Proterozoic Duck Creek Dolomite, Western Australia. Precambrian Res. 38, 257–279.
Knoll, A.H., Javaux, E.J., Hewitt, D., Cohen, P., 2006. Eukaryotic organisms in Proterozoic oceans. Philos. Trans. R. Soc. B-Biol. Sci. 361, 1023–1038.
Knoll, A.H., Summons, R.E., Waldbauer, J.R., Zumberge, J.E., 2007. The geological succession of primary producers in the oceans. In: Falkowski, P.G., Knoll, A.H. (Eds.), Evolution of Primary Producers in the Sea. Academic Press, pp. 133–163.
Knoll, A.H., Worndle, S., Kah, L.C., 2013. Covariance of microfossil assemblages and microbialite textures across an upper Mesoproterozoic carbonate platform. PALAIOS 28, 453–470.
Knoll, A.H., Bergmann, K.D., Strauss, J.V., 2016. Life: the first two billion years. Philos. Trans. R. Soc. B-Biol. Sci. 371, 20150493.
Koëhler, I., Konhauser, K.O., Papineau, D., Bekker, A., Kappler, A., 2013. Biological carbon precursor to diagenetic siderite with spherical structures in iron formations. Nat. Commun. 4, 1741.
Konhauser, K.O., 2007. Introduction to Geomicrobiology. Wiley-Blackwell.
Konhauser, K.O., Pecoits, E., Lalonde, S.V., Papineau, D., Nisbet, E.G., Barley, M.E., Arndt, N.T., Zahnle, K., Kamber, B.S., 2009. Oceanic nickel depletion and a methanogen famine before the great oxidation event. Nature 458, 750–753.
Krumbein, W.E., 2010. Gunflint Chert microbiota revisited - neither stromatolites, nor cyanobacteria. In: Seckbach, J., Oren, A. (Eds.), Microbial Mats: Modern and Ancient Microorganisms in Stratified Systems, Cellular Origin, Life in Extreme Habitats and Astrobiology. Springer, Heidelberg, pp. 53–70.
Kump, L.R., Barley, M.E., 2007. Increased subaerial volcanism and the rise of atmospheric oxygen 2.5 billion years ago. Nature 448, 1033–1036.
Laflamme, M., Schiffbauer, J.D., Dornbos, S.Q. (Eds.), 2011. Quantifying the Evolution of Early Life. Springer, Berlin.
Lalonde, S.V., Konhauser, K.O., 2015. Benthic perspective on Earth's oldest evidence for oxygenic photosynthesis. Proc. Natl. Acad. Sci. U. S. A. 112, 995–1000.
Lamb, D.M., Awramik, S.M., Chapman, D.J., Zhuc, S., 2009. Evidence for eukaryotic diversification in the ~1800 million-year-old Changzhougou formation, North China. Precambrian Res. 173, 93–104.
Lan, Z., Li, X., Chen, Z.-Q., Li, Q., Hofmann, A., Zhang, Y., Zhong, Y., Liu, Y., Tang, G., Ling, X., Li, J., 2014. Diagenetic xenotime age constraints on the Sanjiaotang Formation, Luoyu Group, southern margin of the North China Craton: implications for regional stratigraphic correlation and early evolution of eukaryotes. Precambrian Res. 251, 21–32.
Lanier, W.P., 1989. Interstitial and peloid microfossils from the 2.0 Ga Gunflint Formation: implications for the paleoecology of the Gunflint stromatolites. Precambrian Res. 45, 291–318.
Lekele Baghekema, S.G., Lepot, K., Riboulleau, A., Fadel, A., Trentesaux, A., El Albani, A., 2017. Nanoscale analysis of preservation of ca. 2.1 Ga old Francevillian microfossils, Gabon. Precambrian Res. 301, 1–18.
Lemelle, L., Labrot, P., Salome, M., Simionovici, A., Viso, M., Westall, F., 2008. Situ imaging of organic sulfur in 700–800 My-old Neoproterozoic microfossils using X-ray spectromicroscopy at the SK-edge. Org. Geochem. 39, 188–202.
León-Tejera, H., Pérez-Estrada, C.J., Montejano, G., Serviere-Zaragoza, E., 2011. Biodiversity and temporal distribution of Chroococcales (Cyanoprokaryota) of an arid mangrove on the east coast of Baja California Sur, Mexico. Fottea 11, 235–244.
Lepot, K., 2011. Microfossils, analytical techniques. In: Gargaud, M. (Ed.), Encyclopedia of Astrobiology. Springer, Berlin, pp. 1049–1054.
Lepot, K., Benzerara, K., Brown, G.E., Philippot, P., 2008. Microbially influenced formation of 2,724 million years old stromatolites. Nat. Geosci. 1, 118–121.
Lepot, K., Benzerara, K., Rividi, N., Cotte, M., Brown, G.E., Philippot, P., 2009a. Organic matter heterogeneities in 2.72 Ga stromatolites: alteration versus preservation by sulphur incorporation. Geochim. Cosmochim. Acta 73, 6579–6599.
Lepot, K., Philippot, P., Benzerara, K., Wang, G.Y., 2009b. Garnet-filled trails associated with carbonaceous matter mimicking microbial filaments in Archean basalt. Geobiology 7, 6579–6599.
Lepot, K., Williford, K.H., Ushikubo, T., Sugitani, K., Mimura, K., Spicuzza, M.J., Valley, J.W., 2013. Texture-specific isotopic compositions in 3.4 Gyr old organic matter support selective preservation in cell-like structures. Geochim. Cosmochim. Acta 112, 66–86.
Lepot, K., Compère, P., Gérard, E., Namsaraev, Z., Verleyen, E., Tavernier, I., Hodgson, D.A., Vyverman, W., Gilbert, B., Wilmotte, A., Javaux, E.J., 2014. Organic and mineral imprints in fossil photosynthetic mats of an East Antarctic lake. Geobiology 12, 424–450.
Lepot, K., Addad, A., Knoll, A.H., Wang, J., Troadec, D., Béché, A., Javaux, E.J., 2017. Iron minerals within specific microfossil morphospecies of the 1.88 Ga Gunflint Formation. Nat. Commun. 8, 14890.
Li, H., Lu, S., Su, W., Xiang, Z., Zhou, H., Zhang, Y., 2013. Recent advances in the study of the Mesoproterozoic geochronology in the North China Craton. J. Asia Earth Sci. 72, 216–227.

Licari, G.R., Cloud Jr., P.E., 1968. Reproductive structures and taxonomic affinities of some nanofossils from the Gunflint Iron Formation. Proc. Natl. Acad. Sci. U. S. A. 59, 1053–1060.
Licari, G.R., Cloud, P., 1972. Prokaryotic algae associated with Australian Proterozoic stromatolites. Proc. Natl. Acad. Sci. U. S. A. 69, 2500–2504.
Livage, J., 2009. Chemical synthesis of biomimetic forms. C. R. Palevol 8, 629–636.
Lopez-Garcia, P., Moreira, D., 2015. Open questions on the origin of eukaryotes. Trends Ecol. Evol. 30, 697–708.
Love, G.D., Grosjean, E., Stalvies, C., Fike, D.A., Grotzinger, J.P., Bradley, A.S., Kelly, A.E., Bhatia, M., William, M., Snape, C.E., Bowring, S.A., Condom, D.J., Summons, R., 2009. Fossil steroids record the appearance of Demospongiae during the Cryogenian period. Nature 457, 718–721.
Lyons, T.W., Reinhard, C.T., Planavsky, N.J., 2014. The rise of oxygen in Earth's early ocean and atmosphere. Nature 506, 307–315.
Maliva, R.G., Knoll, A.H., Simonson, B.M., 2005. Secular change in the Precambrian silica cycle: insights from chert petrology. Geol. Soc. Am. Bull. 117, 835–845.
Marshall, C.P., Javaux, E.J., Knoll, A.H., Walter, M.R., 2005. Combined micro-Fourier transform infrared (FTIR) spectroscopy and micro-Raman spectroscopy of Proterozoic acritarchs: a new approach to Palaeobiology. Precambrian Res. 138, 208–224.
Martindale, R.C., Strauss, J.V., Sperling, E.A., Johnson, J.E., Van Kranendonk, M.J., Flannery, D., French, K., Lepot, K., Mazumder, R., Rice, M.S., Schrag, D.P., Summons, R., Walter, M., Abelson, J., Knoll, A.H., 2015. Sedimentology, chemostratigraphy, and stromatolites of lower Paleoproterozoic carbonates, Turee Creek Group, Western Australia. Precambrian Res. 266, 194–211.
Matz, M.V., Frank, T.M., Marshall, N.J., Widder, E.A., Johnsen, S., 2008. Giant deep-sea protist produces bilaterian-like traces. Curr. Biol. 18, 1849–1854.
Melezhik, V.A., Fallick, A.E., Makarikhin, V.V., Lyubtsov, V.V., 1997. Links between Palaeoproterozoic palaeogeography and rise and decline of stromatolites: Fennoscandian shield. Precambrian Res. 82, 311–348.
Melezhik, V.A., Fallick, A.E., Martin, A.P., Condon, D.J., Kump, L.R., Brasier, A.T., 2013. The greatest perturbation of the global carbon cycle: the Lomagundi-Jatuli isotopic event. In: Melezhik, V., Prave, A.R., Hanski, E.J., Fallick, A.E., Lepland, A., Kump, L.R., Strauss, H. (Eds.), Reading the Archive of Earth's Oxygenation. Frontiers in Earth Sciences. Springer, Heidelberg, pp. 1111–1150.
Mendelson, C.V., Schopf, J.W., 1992. Proterozoic and selected Early Cambrian microfossils and microfossil-like objects. In: Schopf, J.W., Klein, C. (Eds.), The Proterozoic Biosphere, A Multidisciplinary Study. Cambridge University Press, pp. 865–952.
Mentel, M., Martin, W., 2008. Energy metabolism among eukaryotic anaerobes in light of Proterozoic ocean chemistry. Philos. Trans. R. Soc. B-Biol. Sci. 363, 2717–2729.
Mloszewska, A.M., Owttrim, G.W., Whitford, D.S., Lalonde, S.V., Kappler, A., Konhauser, K.O., 2015. In: Silica saved our earliest cyanobacteria. Goldschmidt 2015 Conference Abstracts. pp. 2153.
Moczydłowska, M., Willman, S., 2009. Ultrastructure of cell walls in ancient microfossils as a proxy to their biological affinities. Precambrian Res. 173, 27–38.
Moczydłowska, M., Landing, E.D., Zang, W., Palacios, T., 2011. Proterozoic phytoplankton and timing of chlorophyte algae origins. Palaeontology 54 (4), 721–733.
Morad, S., 1990. Mica alteration reactions in Jurassic reservoir sandstones from the Haltenbanken Area, Offshore Norway. Clay Clay Miner. 38, 584–590.
Moreau, J.W., Sharp, T.G., 2004. A transmission electron microscopy study of silica and kerogen biosignatures in-1.9 Ga gunflint microfossils. Astrobiology 4, 196–210.
Muir, M.D., 1983. Proterozoic microfossils from the Mara Dolomite Member, Emmerugga Dolomite, McArthur Group, from the Northern Territory, Australia. Bot. J. Linn. Soc. 86, 1–18.
Mulholland, D.S., Poitrasson, F., Shirokova, L.S., González, A.G., Pokrovsky, O.S., Boaventura, G.R., Vieira, L.C., 2015. Iron isotope fractionation during Fe(II) and Fe (III) adsorption on cyanobacteria. Chem. Geol. 400, 24–33.
Nagovitsin, K.E., Stanevich, A.M., Kornilova, T.A., 2010. Stratigraphic setting and age of the complex Tappania-bearing Proterozoic fossil biota of Siberia. Russ. Geol. Geophys. 51, 1192–1198.
Noffke, N., Christian, D., Wacey, D., Hazen, R.M., 2013a. Microbially induced sedimentary structures recording an ancient ecosystem in the ca. 3.48 billion-year-old dresser formation, Pilbara, Western Australia. Astrobiology 13, 1103–1124.
Noffke, N., Decho, A.W., Stoodley, P., 2013b. Slime through time: the fossil record of prokaryote evolution. PALAIOS 28, 1–5.
Oehler, J.H., 1976. Hydrothermal crystallization of silica gel. Geol. Soc. Am. Bull. 87, 1143–1152.
Oehler, J.H., 1977. Microflora of the HYC pyritic shale member of the Barney Creek formation (McArthur group), middle Proterozoic of northern Australia. Alcheringa 1, 315–349.
Oehler, D.Z.C.,.S.L., 2014. Biogenicity and syngeneity of organic matter in ancient sedimentary rocks: recent advances in the search for evidence of past life. Challenges 5, 260–283.
Oehler, D.Z., Robert, F., Mostefaoui, S., Meibom, A., Selo, M., McKay, D.S., 2006. Chemical mapping of proterozoic organic matter at submicron spatial resolution. Astrobiology 6, 838–850.
Ono, S., Beukes, N.J., Rumble, D., Fogel, M.L., 2006. Early evolution of atmospheric oxygen from multiple-sulfur and carbon isotope records of the 2.9 Ga Mozaan Group of the Pongola Supergroup, Southern Africa. S. Afr. J. Geol. 109, 97–108.
Pace, N.R., 1997. A molecular view of microbial diversity and the biosphere. Science 276, 734–740.
Pang, K., Tang, Q., Schiffbauer, J.D., Yao, J., Yuan, X., Wan, B., Chen, L., Ou, Z., Xiao, S., 2013. The nature and origin of nucleus-like intracellular inclusions in Paleoproterozoic eukaryote microfossils. Geobiology 11, 499–510.
Pang, K., Tang, Q., Yuan, X.L., Wan, B., Xiao, S.H., 2015. A biomechanical analysis of the early eukaryotic fossil Valeria and new occurrence of organic-walled microfossils from the Paleo-Mesoproterozoic Ruyang Group. Palaeoworld 24, 251–262.
Papineau, D., Purohit, R., Fogel, M.L., Shields-Zhou, G.A., 2013. High phosphate availability as a possible cause for massive cyanobacterial production of oxygen in the Paleoproterozoic atmosphere. Earth Planet. Sci. Lett. 362, 225–236.
Papineau, D., de Gregorio, B., Fearn, S., Kilcoyne, D., McMahon, G., Purohit, R., Fogel, M., 2016. Nanoscale petrographic and geochemical insights on the origin of the Palaeoproterozoic stromatolitic phosphorites from Aravalli Supergroup, India. Geobiology 14, 3–32.
Parfrey, L.W., Lahr, D.J.G., Knoll, A.H., Katz, L.A., 2011. Estimating the timing of early eukaryotic diversification with multigene molecular clocks. Proc. Natl. Acad. Sci. U. S. A. 108, 13624–13629.
Parize, O., Feybesse, J.L., Guillocheau, F., Mulder, T., 2013. Were the 2.1-Gyr fossil colonial organisms discovered in the Francevillian basin (Palaeoproterozoic, Gabon) buried by turbidites? Compt. Rendus Geosci. 345, 101–110.
Pawlowski, J., Gooday, A.J., 2009. Precambrian biota: Protistan origin of trace fossils? Curr. Biol. 19, R28–30.
Peng, Y.B., Bao, H.M., Yuan, X.L., 2009. New morphological observations for Paleoproterozoic acritarchs from the Chuanlinggou Formation, North China. Precambrian Res. 168, 223–232.
Petrash, D.A., Robbins, L.J., Shapiro, R.S., Mojzsis, S.J., Konhauser, K.O., 2016. Chemical and textural overprinting of ancient stromatolites: timing, processes, and implications for their use as paleoenvironmental proxies. Precambrian Res. 278, 145–160.
Picard, A., Kappler, A., Schmid, G., Quaroni, L., Obst, M., 2015. Experimental diagenesis of organo-mineral structures formed by microaerophilic Fe(II)-oxidizing bacteria. Nat. Commun. 6, 6277.
Picard, A., Obst, M., Schmid, G., Zeitvogel, F., Kappler, A., 2016. Limited influence of Si on the preservation of Fe mineral encrusted microbial cells during experimental diagenesis. Geobiology 14, 276–292.
Planavsky, N., Rouxel, O., Bekker, A., Shapiro, R., Fralick, P., Knudsen, A., 2009. Iron-oxidizing microbial ecosystems thrived in late Paleoproterozoic redox-stratified oceans. Earth Planet. Sci. Lett. 286, 230–242.
Planavsky, N.J., McGoldrick, P., Scott, C.T., Li, C., Reinhard, C.T., Kelly, A.E., Chu, X., 2011. Widespread iron-rich conditions in the mid-Proterozoic ocean. Nature 477, 448–451.
Planavsky, N.J., Asael, D., Hofmann, A., Reinhard, C.T., Lalonde, S.V., Knudsen, A., Wang, X., Ossa, F.O., Pecoits, E., Smith, A.J.B., Beukes, N.J., Bekker, A., Johnson, T.M., Konhauser, K.O., Lyons, T., Rouxel, O.J., 2014. Evidence for oxygenic photosynthesis half a billion years before the great oxidation event. Nat. Geosci. 7, 283–286.
Porter, S.M., 2006. The Proterozoic fossil record of heterotrophic eukaryotes. In: Xiao, S., Kaufman, A.J. (Eds.), Neoproterozoic Geobiology and Paleobiology. Springer, the Netherlands, pp. 1–21.
Porter, S., 2011. The rise of predators. Geology 39, 607–608.
Porter, S.M., 2016. Tiny vampires in ancient seas: evidence for predation via perforation in fossils from the 780–740 million-year-old Chuar Group, Grand Canyon, USA. Philos. Trans. R. Soc. B-Biol. Sci. 283.
Poulton, S.W., Fralick, P.W., Canfield, D.E., 2010. Spatial variability in oceanic redox structure 1.8 billion years ago. Nat. Geosci. 3, 486–490.
Prasad, B., Asher, R., 2001. Acritarch biostratigraphy and lithostratigraphic classification of Proterozoic and lower Paleozoic sediments (Preunconformity sequence) of Ganga Basin, India. Paleontographica. Indica 5, 151.
Prasad, B., Uniyal, S.N., Asher, R., 2005. Organic-walled microfossils from the Proterozoic Vindhyan Supergroup of Son Valley, Madhya Pradesh, India. Palaeobotanist 54, 13–60.
Rasmussen, B., Fletcher, I.R., Brocks, J.J., Kilburn, M.R., 2008. Reassessing the first appearance of eukaryotes and cyanobacteria. Nature 455, 1101–1104.
Rasmussen, B., Fletcher, I.R., Bekker, A., Muhling, J.R., Gregory, C.J., Thorne, A.M., 2012. Deposition of 1.88-billion-year-old iron formations as a consequence of rapid crustal growth. Nature 484, 498–501.
Ratti, S., Knoll, A.H., Giordano, M., 2011. Did sulfate availability facilitate the evolutionary expansion of chlorophyll $a + c$ phytoplankton in the oceans? Geobiology 9, 301–312.
Ray, J.S., Martin, M.W., Veizer, J., Bowring, S.A., 2002. U-Pb zircon dating and Sr isotope systematics of the Vindhyan Supergroup, India. Geology 30, 131–134.
Reddy, S.M., Evans, D.A.D., 2009. Palaeoproterozoic supercontinents and global evolution: correlations from core to atmosphere. Geol. Soc. Lond. Spec. Publ. 323, 1–26.
Reid, R.P., Visscher, P.T., Decho, A.W., Stolz, J.F., Bebout, B.M., Dupraz, C., Macintyre, L.G., Paerl, H.W., Pinckney, J.L., Prufert-Bebout, L., Steppe, T.F., DesMarais, D.J., 2000. The role of microbes in accretion, lamination and early lithification of modern marine stromatolites. Nature 406, 989–992.
Rosing, M.T., Frei, R., 2004. U-rich Archaean sea-floor sediments from Greenland – indications of > 3700 Ma oxygenic photosynthesis. Earth Planet. Sci. Lett. 217, 237–244.
Samuelsson, J., Butterfield, N.J., 2001. Neoproterozoic fossils from the Franklin Mountains, northwestern Canada: stratigraphic and palaeobiological implications. Precambrian Res. 107, 235–251.
Sánchez-Baracaldo, P., 2015. Origin of marine planktonic cyanobacteria. Sci Rep 5, 17418.
Sánchez-Baracaldo, P., Raven, J.A., Pisani, D., Knoll, A.H., 2017. Early photosynthetic eukaryotes inhabited low-salinity habitats. Proc. Natl. Acad. Sci. U. S. A. 114, E7737–E7745.
Schiffbauer, J.D., Xiao, S.H., 2009. Novel application of focused ion beam electron microscopy (FIB-EM) in preparation and analysis of microfossil ultrastructures: a new view of complexity in early eukaryotic organisms. PALAIOS 24, 616–626.
Schiffbauer, J.D., Yin, L.M., Bodnar, R.J., Kaufman, A.J., Meng, F.W., Hu, J., Shen, B., Yuan, X.L., Bao, H.M., Xiao, S.H., 2007. Ultrastructural and geochemical characterization of Archean-Paleoproterozoic graphite particles: implications for recognizing

traces of life in highly metamorphosed rocks. Astrobiology 7, 684–704.
Schiffbauer, J.D., Wallace, A.F., Hunter, J.L., Kowalewski, M., Bodnar, R.J., Xiao, S., 2012. Thermally-induced structural and chemical alteration of organic-walled microfossils: an experimental approach to understanding fossil preservation in metasediments. Geobiology 10, 402–423.
Schirrmeister, B.E., Vos, J.M.d., Antonelli, A., Bagheri, H.C., 2013. Evolution of multicellularity coincided with increased diversification of cyanobacteria and the great oxidation event. Proc. Natl. Acad. Sci. U. S. A. 110, 1791–1796.
Schneider, D.A., Bickford, M.E., Cannon, W.F., Schulz, K.J., Hamilton, M.A., 2002. Age of volcanic rocks and syndepositional iron formations, Marquette Range Supergroup: implications for the tectonic setting of Paleoproterozoic, iron formations of the Lake Superior region. Can. J. Earth Sci. 39, 999–1012.
Schopf, J.W., 1975. Precambrian paleobiology: problems and perspectives. Annu. Rev. Earth Planet. Sci. 3, 213–249.
Schopf, J.W., 1992. Atlas of representative proterozoic microfossils. In: Schopf, J.W., Klein, C. (Eds.), The Proterozoic Biosphere: A Multidisciplinary Study. Cambridge University Press, pp. 1055–1118.
Schopf, J.W., Kudryavtsev, A.B., 2009. Confocal laser scanning microscopy and Raman imagery of ancient microscopic fossils. Precambrian Res. 173, 39–49.
Schopf, J.W., Prasad, K.N., 1978. Microfossils in Collenia-like stromatolites from the Proterozoic Vempalle formation of the Cuddapah basin, India. Precambrian Res. 6, 347–366.
Schopf, J.W., Kudryavtsev, A.B., Agresti, D.G., Czaja, A.D., Wdowiak, T.J., 2005. Raman imagery: a new approach to assess the geochemical maturity and biogenicity of permineralized Precambrian fossils. Astrobiology 5, 333–371.
Schopf, J.W., Kudryavtsev, A.B., Walter, M.R., Van Kranendonk, M.J., Williford, K.H., Kozdon, R., Valley, J.W., Gallardo, V.A., Espinoza, C., Flannery, D.T., 2015. Sulfur-cycling fossil bacteria from the 1.8-Ga Duck Creek formation provide promising evidence of evolution's null hypothesis. Proc. Natl. Acad. Sci. U. S. A. 112, 2087–2092.
Scott, C., Wing, B.A., Bekker, A., Planavsky, N.J., Medvedev, P., Bates, S.M., Yun, M., Lyons, T.W., 2014. Pyrite multiple-sulfur isotope evidence for rapid expansion and contraction of the early Paleoproterozoic seawater sulfate reservoir. Earth Planet. Sci. Lett. 389, 95–104.
Seilacher, A., 2001. Concretion morphologies reflecting diagenetic and epigenetic pathways. Sediment. Geol. 143, 41–57.
Sergeev, V.N., 2009. The distribution of microfossil assemblages in Proterozoic rocks. Precambrian Res. 173, 212–222.
Sergeev, V.N., Gerasimenko, L.M.Z., Zavarzin, G.A., 2002. The Proterozoic history and present state of cyanobacteria. Microbiology 71, 623–637.
Sessions, A.L., Doughty, D.M., Welander, P.V., Summons, R.E., Newman, D.K., 2009. The continuing puzzle of the great oxidation event. Curr. Biol. 19, R567–R574.
Shapiro, R.S., Konhauser, K.O., 2015. Hematite-coated microfossils: primary ecological fingerprint or taphonomic oddity of the Paleoproterozoic? Geobiology 13, 209–224.
Sharma, M., 2006a. Palaeobiology of Mesoproterozoic Salkhan limestone, Semri group, Rohtas, Bihar, India: systematics and significance. J. Earth Syst. Sci. 115, 67–98.
Sharma, M., 2006b. Small-sized akinetes from the Mesoproterozoic Salkhan limestone, Semri group, Bihar, India. J. Palaeontol. Soc. India 51, 109–118.
Sharma, M., Shukla, Y., 2009. Taxonomy and affinity of Early Mesoproterozoic megascopic helically coiled and related fossils from the Rohtas Formation, the Vindhyan Supergroup, India. Precambrian Res. 173, 105–122.
Sharma, M., Mishra, S., Dutta, S., Banerjee, S., Shukla, Y., 2009. On the affinity of Chuaria–Tawuia complex: a multidisciplinary study. Precambrian Res. 173, 123–136.
Sharma, M., Tiwari, M., Ahmad, S., Shukla, R., Shukla, B., Singh, V.K., Kumar, S., 2016. Palaeobiology of Indian Proterozoic and Early Cambrian successions—recent developments. Proc. Indian Natl. Sci. Acad. 82, 559–579.
She, Z., Strother, P., McMahon, G., Nittler, L.R., Wang, J., Zhang, J., Sang, L., Ma, C., Papineau, D., 2013. Terminal Proterozoic cyanobacterial blooms and phosphogenesis documented by the Doushantuo granular phosphorites I: in situ micro-analysis of textures and composition. Precambrian Res. 235, 20–35.
Shen, Y.N., Canfield, D.E., Knoll, A.H., 2002. Middle proterozoic ocean chemistry: evidence from the McArthur Basin, northern Australia. Am. J. Sci. 302, 81–109.
Shen, Y., Knoll, A.H., Walter, M.R., 2003. Evidence for low sulphate and anoxia in a mid-Proterozoic marine basin. Nature 423, 632–635.
Shen, Y., Farquhar, J., Masterson, A., Kaufman, A.J., Buick, R., 2009. Evaluating the role of microbial sulfate reduction in the early Archean using quadruple isotope systematics. Earth Planet. Sci. Lett. 279, 383–391.
Shi, M., Feng, Q.-L., Khan, M.Z., Awramik, S., Zhu, S.-X., 2017. Silicified microbiota from the Paleoproterozoic Dahongyu Formation, Tianjin, China. J. Paleontol. 91, 369–392.
Shih, P.M., Hemp, J., Ward, L.M., Matzke, N.J., Fischer, W.W., 2017. Crown group Oxyphotobacteria postdate the rise of oxygen. Geobiology 15, 19–29.
Siegel, B.Z., Siegel, S.M., 1970. Biology of the Precambrian genus Kakabekia: new oservations on living Kakabekia barghoorniana. Proc. Natl. Acad. Sci. U. S. A. 67, 1005–1010.
Singh, V.K., Sharma, M., 2014. Palaeoproterozoic-Early Mesoprotreozoic Chitrakut Formation, Vindhyan Supergroup, central India and their implications on the antiquity of eukaryotes. J. Palaeontol. Soc. India 59, 89–102.
Slotznick, S.P., Fischer, W.W., 2016. Examining Archean methanotrophy. Earth Planet. Sci. Lett. 441, 52–59.
Sommers, M.G., Awramik, S.M., Woo, K.S., 2000. Evidence for initial calcite-aragonite composition of lower algal Chert member ooids and stromatolites, Paleoproterozoic Gunflint Formation, Ontario, Canada. Can. J. Earth Sci. 37, 1229–1243.
Spang, A., Ettema, T.J.G., 2016. Microbial diversity: the tree of life comes of age. Nat. Microbiol. 1.
Sperling, E.A., Frieder, C.A., Raman, A.V., Girguis, P.R., Levin, L.A., Knoll, A.H., 2013. Oxygen, ecology, and the Cambrian radiation of animals. Proc. Natl. Acad. Sci. U. S. A. 110, 13446–13451.
Steemans, P., Lepot, K., Marshall, C.P., Hérissé, A.L., Javaux, E., 2010. FTIR characterisation of the chemical composition of Silurian miospores (cryptospores and trilete spores) from Gotland, Sweden. Rev. Palaeobot. Palynol. 162, 577–590.
Stolz, J.F., Feinstein, T.N., Salsi, J., Visscher, P.T., Reid, R.P., 2001. TEM analysis of microbial mediated sedimentation and lithification in modern marine stromatolites. Am. Mineral. 86, 826–833.
Storme, J.Y., Golubic, S., Wilmotte, A., Kleinteich, J., Velazquez, D., Javaux, E.J., 2015. Raman characterization of the UV-protective pigment gloeocapsin and its role in the survival of cyanobacteria. Astrobiology 15, 843–857.
Strother, P.K., Tobin, K., 1987. Observations on the genus Huroniospora Barghoorn: implications for paleoecology of the Gunflint microbiota. Precambrian Res. 36, 323–333.
Stüeken, E.E., Buick, R., Guy, B.M., Koehler, M.C., 2015. Isotopic evidence for biological nitrogen fixation by molybdenum-nitrogenase from 3.2 Gyr. Nature 520, 666–669.
Su, W., Li, H., Xu, L., Jia, S., Geng, J., Zhou, H., Wang, Z., Pu, H.-Y., 2012. Luoyu and Ruyang Group at the south margin of the North China Craton (NCC) should belong in the Mesoproterozoic Changchengian System: direct constraints from the LA-MC-ICPMS U-Pb age of the tuffite in the Luoyukou Formation, Ruzhou, Henan, China. Geol. Surv. Res. 35, 96–108.
Summons, R.E., Walter, M.R., 1990. Molecular fossils and microfossils of prokaryotes and protists from Proterozoic sediments. Am. J. Sci. 290, 212–244.
Swanner, E.D., Wu, W., Hao, L., Wüstner, M.L., Obst, M., Moran, D.M., McIlvin, M.R., Saito, M.A., Kappler, A., 2015. Physiology, Fe(II) oxidation, and Fe mineral formation by a marine planktonic cyanobacterium grown under ferruginous conditions. Front. Earth Sci. 3, 60.
Talyzina, N.M., Moczydłowska, M., 2000a. Morphological and ultrastructural studies of some acritarchs from the lower Cambrian Lukati formation, Estonia. Rev. Palaeobot. Palynol. 112, 1–21.
Talyzina, N.M., Moczydłowska, M., 2000b. Morphological and ultrastructural studies of some acritarchs from the lower Cambrian Lükati formation, Estonia. Rev. Palaeobot. Palynol. 112, 1–21.
Tang, Q., Pang, K., Yuan, X., Xiao, S., 2017. Electron microscopy reveals evidence for simple multicellularity in the Proterozoic fossil Chuaria. Geology 45, 75–78.
Tappan, H., 1976. Possible eukaryotic algae (Bangiophycidae) among Early Proterozoic microfossils. Geol. Soc. Am. Bull. 87, 633–639.
Thomazo, C., Ader, M., Philippot, P., 2011. Extreme 15N-enrichments in 2.72-Gyr-old sediments: evidence for a turning point in the nitrogen cycle. Geobiology 9, 107–120.
Timofeev, B.V., 1966. Micropaleophytological Investigations of Ancient Suites. Nauka, Moscow.
Timofeev, B.V., 1982. Microphytofossils of the Early Precambrian. “Nauka”, Leningrad.
Tomitani, A., Knoll, A.H., Cavanaugh, C.M., Ohno, T., 2006. The evolutionary diversification of cyanobacteria: molecular-phylogenetic and paleontological perspectives. Proc. Natl. Acad. Sci. U. S. A. 103, 5442–5447.
Tyler, S.A., Barghoorn, E.S., 1954. Occurrence of structurally preserved plants in pre-Cambrian rocks of the Canadian shield. Science 119, 606–608.
Ueno, Y., Yamada, K., Yoshida, N., Maruyama, S., Isozaki, Y., 2006. Evidence from fluid inclusions for microbial methanogenesis in the early Archaean era. Nature 440, 516–519.
Ueno, Y., Ono, S., Rumble, D., Maruyama, S., 2008. Quadruple sulfur isotope analysis of ca. 3.5 Ga dresser formation: new evidence for microbial sulfate reduction in the early Archean. Geochim. Cosmochim. Acta 72, 5675–5691.
Van Kranendonk, M.J., Schopf, J.W., Grice, K., Walter, M., Pages, A., Kudryavtsev, A.B., Gallardo, V.A., Espinoza, C., Melendez, I., Lepland, A., 2012. In: A 2.3 Ga sulfuretum at the GOE: microfossil and organic geochemistry evidence from the Turee Creek Group, Western Australia. AbSciCon Conference, Atlanta. . http://abscicon2012.arc.nasa.gov/abstracts/.
Van Zuilen, M.A., Lepland, A., Arrhenius, G., 2002. Reassessing the evidence for the earliest traces of life. Nature 420, 627–630.
Vasconcelos, C., Warthmann, R., McKenzie, J.A., Visscher, P.T., Bittermann, A.G., van Lith, Y., 2006. Lithifying microbial mats in Lagoa Vermelba, Brazil: modern Precambrian relics? Sediment. Geol. 185, 175–183.
Wacey, D., Menon, S., Green, L., Gerstmann, D., Kong, C., Mcloughlin, N., Saunders, M., Brasier, M., 2012. Taphonomy of very ancient microfossils from the ~3400 Ma Strelley Pool Formation and ~1900 Ma Gunflint Formation: new insights using a focused ion beam. Precambrian Res. 220-221, 234–250.
Wacey, D., McLoughlin, N., Kilburn, M.R., Saunders, M., Cliff, J.B., Kong, C., Barley, M.E., Brasier, M.D., 2013. Nanoscale analysis of pyritized microfossils reveals differential heterotrophic consumption in the ~1.9-Ga Gunflint chert. Proc. Natl. Acad. Sci. U. S. A. 110, 8020–8024.
Wacey, D., Battison, L., Garwood, R.J., Hickman-Lewis, K., Brasier, M.D., 2016. Advanced analytical techniques for studying the morphology and chemistry of Proterozoic microfossils. In: Brasier, A.T., McIlroy, D., McLoughlin, N. (Eds.), Earth System Evolution and Early Life: A Celebration of the Work of Martin Brasier. Special Publications. Geological Society, London.
Waldbauer, J.R., Newman, D.K., Summons, R.E., 2011. Microaerobic steroid biosynthesis and the molecular fossil record of Archean life. Proc. Natl. Acad. Sci. U. S. A. 108, 13409–13414.
Walter, M.R., Bauld, J., Brock, T.D., 1976a. Microbiology and morphogenesis of columnar stromatolites (Conophyton, Vacerrilla) from hot springs in Yellowstone National Park. In: Walter, M.R. (Ed.), Stromatolites. Elsevier, New York, pp. 273–310.
Walter, M.R., Goode, D.T., Hall, W.D.M., 1976b. Microfossils from a newly discovered Precambrian stromatolitic iron formation in Western Australia. Nature 261, 221–223.
Waterbury, J.B., Stanier, R.Y., 1978. Patterns of growth and development in Pleurocapsalean cyanobacteria. Microbiol. Rev. 42, 2–44.
Weber, F., Gauthier-Lafaye, F., 2013. No proof from carbon isotopes in the Francevillian

(Gabon) and Onega (Fennoscandian shield) basins of a global oxidation event at 1980–2090 Ma following the great oxidation event (GOE). C. R. Geoscience 345, 28–35.
Westall, F., Folk, R.L., 2003. Exogenous carbonaceous microstructures in Early Archaean cherts and BIFs from the Isua Greenstone Belt: implications for the search for life in ancient rocks. Precambrian Res. 126, 313–330.
Williford, K.H., Ushikubo, T., Schopf, J.W., Lepot, K., Kitajima, K., Valley, J.W., 2013. Preservation and detection of microstructural and taxonomic correlations in the carbon isotopic compositions of individual Precambrian microfossils. Geochim. Cosmochim. Acta 104, 165–182.
Willman, S., Cohen, P.A., 2011. Ultrastructural approaches to the microfossil record: assessing biological affinities by use of Transmission Electron Microscopy. In: Laflamme, M., Schiffbauer, J.D., Dornbos, S.Q. (Eds.), Quantifying the Evolution of Early Life. Topics in Geobiology. Springer, Berlin, pp. 301–320.
Wilson, J.P., Fischer, W.W., Johnston, D.T., Knoll, A.H., Grotzinger, J.P., Walter, M.R., McNaughton, N.J., Simon, M., Abelson, J., Schrag, D.P., Summons, R., Allwood, A., Andres, M., Gammon, Crystal, Garvin, J., Rashby, S., Schweizer, M., Watters, W.A., 2010. Geobiology of the late Paleoproterozoic Duck Creek Formation, Western Australia. Precambrian Res. 179, 135–149.
Wood, S.A., Paul, W.J., Hamilton, D.P., 2008. Cyanobacterial biovolumes for the Rotorua lakes. Cawthron Rep. 1054.
Xiao, S., Dong, L., 2006. On the morphological and ecological history of Proterozoic macroalgae. In: Xiao, S., Kaufman, A.J. (Eds.), Neoproterozoic Geobiology and Paleobiology. Springer, pp. 57–90.
Xiao, S.H., Knoll, A.H., Kaufman, A.J., Yin, L.M., Zhang, Y., 1997. Neoproterozoic fossils in Mesoproterozoic rocks? Chemostratigraphic resolution of a biostratigraphic conundrum from the north China platform. Precambrian Res. 84, 197–220.
Yin, L.M., 1997. Acanthomorphic acritarchs from meso-neoproterozoic shales of the Ruyang Group, Shanxi, China. Rev. Palaeobot. Palynol. 98, 15–25.
Yin, L.M., Yuan, X.L., Meng, F.W., Hu, J., 2005. Protists of the Upper Mesoproterozoic Ruyang Group in Shanxi Province, China. Precambrian Res. 141, 49–66.
Yun, Z., 1984. A Gunflint type of microfossil assemblage from early Proterozoic stromatolitic cherts in China. Nature 309, 547–549.
Zhang, Z., 1986. Clastic facies microfossils from the Chuanlinggou Formation (1800 Ma) near Jixian, North China. J. Micropalaentol. 5, 9–16.
Zhang, Y., Golubic, S., 1987. Endolithic microfossils (Cyanophyta) from early Proterozoic stromatolites, Hebei, China. Acta Micropalaeo. Sin. 4, 1–12.
Zhu, S.X., Zhu, M.Y., Knoll, A.H., Yin, Z.J., Zhao, F.C., Sun, S.F., Qu, Y.G., Shi, M., Liu, H., 2016. Decimetre-scale multicellular eukaryotes from the 1.56-billion-year-old Gaoyuzhuang Formation in North China. Nat. Commun. 7.